ISTANBUL TECHNICAL UNIVERSITY ★ GRADUATE SCHOOL

DESIGN OF AN OFFSHORE WIND FARM OFF DİKİLİ SHORES

M.Sc. THESIS

Erdem ACAR

Department of Shipbuilding and Ocean Engineering

Offshore Engineering Programme

JULY 2021

ISTANBUL TECHNICAL UNIVERSITY ★ GRADUATE SCHOOL

DESIGN OF AN OFFSHORE WIND FARM OFF DİKİLİ SHORES

M.Sc. THESIS

Erdem ACAR
(508171205)

Department of Shipbuilding and Ocean Engineering

Offshore Engineering Programme

Thesis Advisor: Prof. Dr. Serdar BEJİ

JULY 2021

İSTANBUL TEKNİK ÜNİVERSİTESİ ★ LİSANSÜSTÜ EĞİTİM ENSTİTÜSÜ

DİKİLİ AÇIKLARINDA BİR AÇIK DENİZ RÜZGAR ÇİFTLİĞİ TASARIMI

YÜKSEK LİSANS TEZİ

Erdem ACAR
(508171205)

Gemi ve Deniz Teknolojisi Mühendisliği Anabilim Dalı

Açık Deniz Mühendisliği Programı

Tez Danışmanı: Prof. Dr. Serdar BEJİ

TEMMUZ 2021

Erdem ACAR, a M.Sc. student of ITU Graduate School student ID **508171205**, successfully defended the thesis entitled "**DESIGN OF AN OFFSHORE WIND FARM OFF DİKİLİ SHORES**", which he prepared after fulfilling the requirements specified in the associated legislations, before the jury whose signatures are below.

Thesis Advisor :	**Prof. Dr. Serdar BEJİ** Istanbul Technical University	.....
Jury Members :	**Prof. Dr. Yalçın YÜKSEL** Yildiz Technical University	.....
	Dr. Deniz BAYRAKTAR BURAL Istanbul Technical University	.....

Date of Submission : 16 June 2021
Date of Defense : 05 July 2021

In memory of my father Necdet ACAR (1940-2020),

FOREWORD

Wind has been used as an energy source for centuries. Wind has no cost as a primary energy source. Wind energy does not produce air pollution, acid rain, carbon emissions, and radioactive waste. Wind energy potential is much higher than current energy consumption in the world. Wind energy is advantageous compared to other renewable energy sources because it is already operational and the wind power industry has gained a great deal of experience from the design and operation of wind farms in the last thirty years. Therefore, more attention should be paid to wind power generation.

I would like to thank my advisor Prof. Dr. Serdar BEJİ for his guidance in this thesis.

June 2021

Erdem ACAR
Naval Architect and Ocean Engineer

TABLE OF CONTENTS

Page

ABBREVIATIONS

AWS : Automatic Weather Station
EGDI : European Geological Data Infrastructure
EIA : Energy Information Administration
GWA : Global Wind Atlas
IEC : International Electrotechnical Commission
NNE : North-North-East
OWE : Offshore Wind Energy
OWF : Offshore Wind Farm
OWT : Offshore Wind Turbine
pdf : probability density function
RNA : Rotor-Nacelle Assembly
SSW : South-South-West
SWL : Still Water Level
WTGS : Wind Turbine Generator System

SYMBOLS

A	**:** Area
a	**:** Wave amplitude
C	**:** Weibull scale parameter
C_d	**:** Drag coefficient
C_m	**:** Inertia coefficient
C_p	**:** Power coefficient
c	**:** Wave celerity (speed)
cf	**:** Capacity factor
D	**:** Diameter
d	**:** Water depth
E	**:** Energy
F	**:** Fetch
F_d	**:** Drag force
F_i	**:** Inertia force
H	**:** Wave height
H_s	**:** Significant wave height
h	**:** Height
h_{ref}	**:** Reference height
I_u	**:** Turbulence intensity
K	**:** Weibull shape parameter
k	**:** Wave number
L	**:** Wavelength
M_d	**:** Drag moment
M_i	**:** Inertia moment
$\dot{m}$	**:** Mass flow rate
P	**:** Power
T	**:** Wave period
T_s	**:** Significant wave period
t	**:** Time
U	**:** Wind speed

U_A : Adjusted wind speed

U_{ave} : Average wind speed

U_f : Fastest mile wind speed

U_{ref} : Reference wind speed

U_{3600} : 1-hour average wind speed

u : Water velocity

x : Direction of wave motion

z : Distance up from SWL

z_0 : Roughness length

ζ : Wave profile

ρ : Seawater density

ρ_a : Air density

ω : Circular frequency

LIST OF TABLES

Page

LIST OF FIGURES

Page

DESIGN OF AN OFFSHORE WIND FARM OFF DİKİLİ SHORES

SUMMARY

In this thesis, a potential offshore wind farm (OWF) off Dikili shores was technically designed. The purpose of this thesis is emphasize to the importance of the offshore wind potential of Turkey and give an example to the use of this potential with a case study.

In Turkey, there have been installed many onshore wind farms but has not yet been installed an OWF. The construction and installation costs of OWFs are higher than onshore wind farms. It is also crucial to select the appropriate offshore wind turbine (OWT) model. Because there are many differences between OWTs and land-based wind turbines. With the increasing size and efficiency of wind turbines, the use of offshore wind energy is gaining momentum. Additionally, the offshore wind industry is expanding with the advances in technology are reducing costs and increasing the installation of OWFs. The use of OWE is expected to continue to increase significantly in the near future with the installation of more efficient wind turbines, thus reducing OWE costs.

In this thesis, the "Horns Rev I wind farm" that is the first large-scale OWF in the world located on the west coast of Denmark is used as the reference OWF. The site selected for the OWF is the southwestern shores of Dikili. The location of the OWF is opposite the Island of Karaada that is located in the Bay of Narlidere in the Gulf of Candarli. There is no meteorological observation station in the seas of Turkey. The nearest meteorological observation station to the location of the OWF is Dikili Automatic Weather Station is 19.7 km distance from the center of the OWF. However, the wind data of Karaada that was obtained from the Meteoblue weather archive is used for the OWF. The Meteoblue provides high-quality local weather information for any point in the world, whether on land or at sea. The Meteoblue climate diagrams are based on hourly weather model simulations. From 1985 to 2020, 35-year monthly weather archive diagrams for Karaada are given in Appendix A.

The selected wind turbine for the OWF is "Vestas V80 - 2.0 Offshore" (IEC IIA class) with a hub height of 78 m. The wind farm area consists of ten units OWT in two rows, with five wind turbines per row, and installed power of the OWF is 20 MW. The selected grid connection point is the Port of Narlidere that is the nearest convenient place to the OWF. The selected foundation type for the OWF dependent on the water depth and the seabed conditions is mono-pile foundation. Finally, the maximum total wave force and moment acting on the mono-piles in the OWF were calculated using the Morison equation that can be useful for approximate results.

DİKİLİ AÇIKLARINDA BİR AÇIK DENİZ RÜZGÂR ÇİFTLİĞİ TASARIMI

ÖZET

Bu tez çalışmasında, Dikili kıyıları açıklarında potansiyel bir açık deniz rüzgâr çiftliği teknik olarak tasarlanmıştır. Bu tez çalışmasının amacı ise Türkiye'nin açık deniz rüzgâr potansiyelinin önemini vurgulamak ve bu potansiyelin kullanımına bir vaka çalışması ile örnek vermektir.

Türkiye'de çok sayıda rüzgâr çiftliği kurulmuş ancak henüz bir açık deniz rüzgâr çiftliği kurulmamıştır. Açık deniz rüzgâr çiftliklerinin inşaat ve kurulum maliyetleri, karadaki rüzgâr çiftliklerinden daha yüksektir. Uygun açık deniz rüzgâr türbini modelini seçmek de çok önemlidir. Çünkü açık deniz rüzgâr türbinleri ile kara-temelli rüzgâr türbinleri arasında birçok fark vardır. Rüzgâr türbinlerinin artan boyutu ve verimliliği ile açık deniz rüzgâr enerjisinin kullanımı hız kazanmaktadır. Bununla birlikte, açık deniz rüzgâr endüstrisi teknolojideki gelişmelerle birlikte genişlemekte, maliyetler düşmekte ve açık deniz rüzgâr çiftliklerinin kurulumu artmaktadır. Açık deniz rüzgâr enerjisi kullanımının, yakın gelecekte daha verimli rüzgâr türbinlerinin kurulmasıyla önemli ölçüde artmaya devam etmesi ve böylece açık deniz rüzgâr enerjisi maliyetlerinin azalması beklenmektedir.

Türkiye, özellikle kıyı bölgelerindeki yüksek güç yoğunlukları nedeniyle önemli bir rüzgâr enerjisi potansiyeline sahiptir. Türkiye Rüzgâr Enerjisi Kurumu'na göre, toplam rüzgâr enerjisi kapasitesi 2017 başında 6.1 GW iken, hâlihazırda kurulu rüzgâr enerjisi kapasitesi toplam potansiyelin %7.3'ünü oluşturmaktadır ve bunların hiçbiri de açık deniz rüzgâr projesi değildir. Avrupa ülkeleri ile karşılaştırıldığında Türkiye 83 GW ile sınıf III'ün (yıllık ortalama 7.5 m/s rüzgâr hızı) üzerinde en yüksek rüzgâr enerjisi potansiyeline sahiptir. Marmara bölgesi, yıllık ortalama rüzgâr hızının en yüksek olduğu bölgedir ve onu Ege bölgesi izlemektedir. Ege Denizi ise bugün açık deniz rüzgâr projelerinin yaklaşık %70'inin yer aldığı Kuzey Denizi'ne (50 m yükseklikte 8 m/s'nin üzerinde) benzer rüzgâr hızı profillerine sahiptir. Avrupa Çevre Ajansı tarafından gösterilen önemli açık deniz rüzgâr kapasitesine rağmen Türkiye, bu kapasiteyi henüz kullanmaya başlamamış ülkelerden biridir. Ancak Türkiye'de bir fizibilite çalışmasının yapılması da gerekmektedir.

Türkiye'de açık deniz rüzgârı için en uygun alanlar, rüzgâr hızlarının 9 m/s'ye kadar çıktığı Ege Denizi'nin kuzeybatısındadır. Marmara Denizi ve Karadeniz de 7-8 m/s ile iyi rüzgâr hızlarına sahiptir. Batı kıyılarında birçok fırsat vardır. Su derinliği 50 m'den az olan alanlar, dipten sabitlenmiş temeller için 12 GW açık deniz rüzgâr gücü potansiyeline sahiptir.

Bu tez çalışmasında, Danimarka'nın batı kıyısında yer alan, dünyanın ilk büyük ölçekli açık deniz rüzgâr çiftliği olan “Horns Rev I rüzgâr çiftliği” referans açık deniz rüzgâr çiftliği olarak kullanılmıştır. Açık deniz rüzgâr çiftliği için seçilen yer Dikili'nin güneybatı kıyılarıdır. Açık deniz rüzgâr çiftliğinin konumu, Çandarlı körfezinde Narlıdere koyunda bulunan Karaada'nın karşısındadır. Türkiye denizlerinde meteorolojik gözlem istasyonu bulunmamaktadır. Açık deniz rüzgâr çiftliğinin bulunduğu yere en yakın meteorolojik gözlem istasyonu, açık deniz rüzgâr çiftliği merkezine 19.7 km uzaklıkta bulunan Dikili Otomatik Hava İstasyonudur. Bu nedenle açık deniz rüzgâr çiftliği için Karaada'nın Meteoblue hava durumu arşivinden elde edilen rüzgâr verileri kullanılmıştır. Meteoblue, ister karada ister denizde olsun dünyanın herhangi bir noktası için yüksek kaliteli yerel hava durumu bilgileri sağlamaktadır. Meteoblue iklim diyagramları, saatlik hava modeli simülasyonlarına dayanmaktadır. Karaada için 1985'ten 2020'ye kadar 35 yıllık aylık hava durumu arşiv diyagramları Ek A'da verilmiştir.

Açık deniz rüzgâr çiftliği için seçilen rüzgâr türbini, göbek yüksekliği 78 m olan “Vestas V80 - 2.0 Offshore” (IEC IIA sınıfı)'dur. Rüzgâr çiftliği alanı, sıra başına beş rüzgâr türbini ile iki sıra halinde on ünite açık deniz rüzgâr türbininden oluşmaktadır ve açık deniz rüzgâr çiftliğindeki kurulu güç 20 MW olacaktır. Seçilen şebeke bağlantı noktası, açık deniz rüzgâr çiftliğine en yakın uygun yer olan Narlıdere limanıdır. Açık deniz rüzgâr çiftliği için su derinliğine ve deniz tabanı koşullarına bağlı olarak seçilen temel tipi tek kazıklı (mono-pile) temeldir. Son olarak, açık deniz rüzgâr çiftliğindeki kazıklara etkiyen maksimum toplam dalga kuvveti ve momenti, yaklaşık sonuçlar için faydalı olabilecek Morison denklemi kullanılarak hesaplanmıştır.

1. INTRODUCTION

1.1 Purpose of the Thesis and Literature Review Summary

In this thesis, a potential offshore wind farm (OWF) off Dikili shores was technically designed. The purpose of this thesis is emphasize to the importance of the offshore wind potential of Turkey and give an example to the use of this potential with a case study. As a result of the literature review it has been determined that, there are very few thesis studies on offshore wind energy (OWE) in Turkey.

In Turkey, there have been installed many onshore wind farms but has not yet been installed an OWF. The construction and installation costs of OWFs are higher than onshore wind farms. The installation of the suitable substructure and foundation according to the water depth and the soil conditions on seabed for a potential wind farm area constitute most important part of the total cost.

It is also crucial to select the appropriate offshore wind turbine (OWT) model. Because there are many differences between OWTs and land-based wind turbines. Installation of OWTs involves pre-assembling of the main components on land, transferring and placing them in their offshore location with the various vessels specially designed.

Although offshore wind speeds are generally higher than onshore, this factor have prevented land-based wind turbines from being used offshore in the past. With the increasing size and efficiency of wind turbines, the use of offshore wind energy is gaining momentum.

Improvements to foundation structures of OWTs are subject to research to enable deployment in deeper waters and difficult seabed conditions. Floating supports are the main foundation structures under research for OWTs. Additionally, the offshore wind industry is expanding with the advances in technology are reducing costs and increasing the installation of OWFs.

1.2 Historical Development of Offshore Wind Energy

Wind turbines were developed significantly in the 18th and 19th centuries, and they began to generate electricity in the late 19th century. Development continued unevenly into the 20th century, and in the 1970s, modern wind turbines began to appear. From 1970 to 1990, mainly land-based wind turbines were installed due to economic factors. Capacity was lower and costs higher for OWFs compared to onshore wind farms. The first commercial OWF was installed in 1991 in Vindeby-Denmark, in the Baltic Sea. The Vindeby wind farm (shown in Figure 1.1), which was dismantled in 2017, consisted of eleven marinized land-based wind turbines (total capacity of 5 MW) located between 1.5 and 3 km from the shore.

Figure 1.1 : Vindeby wind farm in Denmark, decommissioned in 2017.

In 2002 and 2003, the first large-scale OWFs were installed in Denmark, with the offshore wind projects at Horns Rev and Nysted. Throughout the 2000s, OWFs continued to expand in the North Sea, Irish Sea, and Baltic Sea. These areas have ideal conditions for OWFs with strong winds (average wind speeds above 8 m/s) and relatively shallow water depths (less than 50 m). Limited progress was made in OWE until 2008, mainly due to high costs and technical complexities. As of 2009, there were over 2 GW of OWT installed in Europe.

In 2017, the United Kingdom hosted the world's largest offshore wind industry with 8.5 GW of cumulative capacity and the lowest cost in the world. As shown in Figure 1.2, Germany, Denmark, Belgium and the Netherlands also contributed significantly to the growth of the European offshore wind market between 2010 and 2018. While the majority with 60% was in Europe, the continent's market dominance has loosened with the high capacity additions in China. As of 2020, global OWE capacity was around 25 GW.

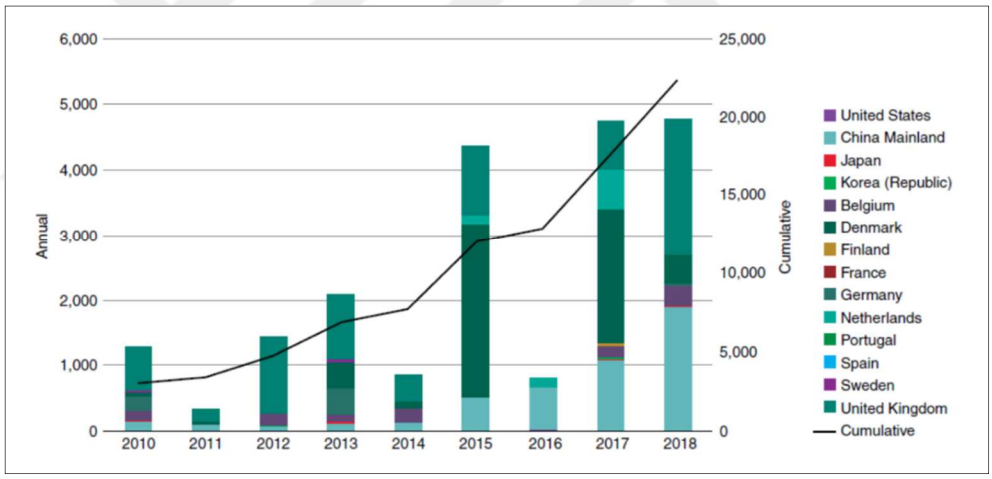

Figure 1.2 : Annual OWF installations by country and cumulative capacity (MW).

OWE is becoming more attractive as technology continues to advance and more wind turbine manufacturers start producing turbines for offshore use. The use of OWE is expected to continue to increase significantly in the near future with the installation of more efficient wind turbines, thus reducing OWE costs.

1.3 Wind Energy in Turkey

Turkey has a significant wind energy potential due to its high power densities, especially in coastal areas. According to the Turkish Wind Energy Association, the cumulative installed wind energy capacity was 6.1 GW at the beginning of 2017. Currently installed wind energy capacity accounts for 7.3% of the total potential, but none of these are from offshore wind projects. Compared to European countries, Turkey has the highest wind energy potential with 83 GW above class III (annual average wind speed of 7.5 m/s). The Marmara region is the region with the highest annual average wind speed, followed by the Aegean region. As shown in Figure 1.3, the Aegean Sea has wind speed profiles similar to the North Sea (above 8 m/s at 50 m height) where approximately 70% of offshore wind projects are located today. Despite the significant offshore wind capacity shown by the European Environment Agency, Turkey is one of the countries that has not yet started to use this capacity. However, a feasibility study needs to be done in Turkey.

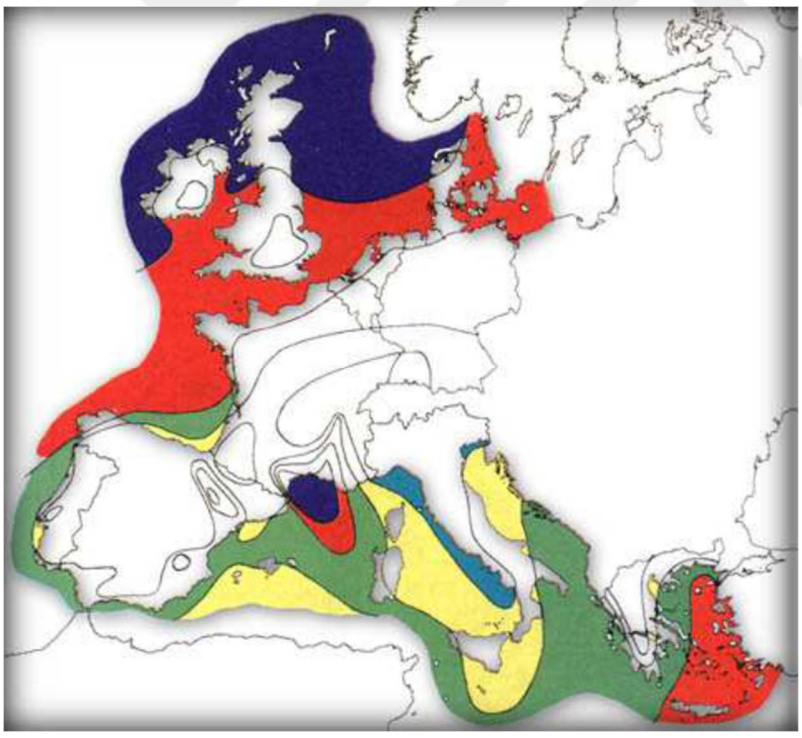

Figure 1.3 : European offshore wind map.

1.3.1 Offshore wind potential

Figure 1.4, which was obtained from the Global Wind Atlas (GWA) and having a coverage area up to 50 km, represents an overview of the annual average wind speed at 50 m height in Turkey. Offshore wind projects are potentially feasible at wind speeds above 7 m/s; these areas are marked with orange and red. However, wind speed is only one of the issues to be considered in determining where offshore wind might prevail.

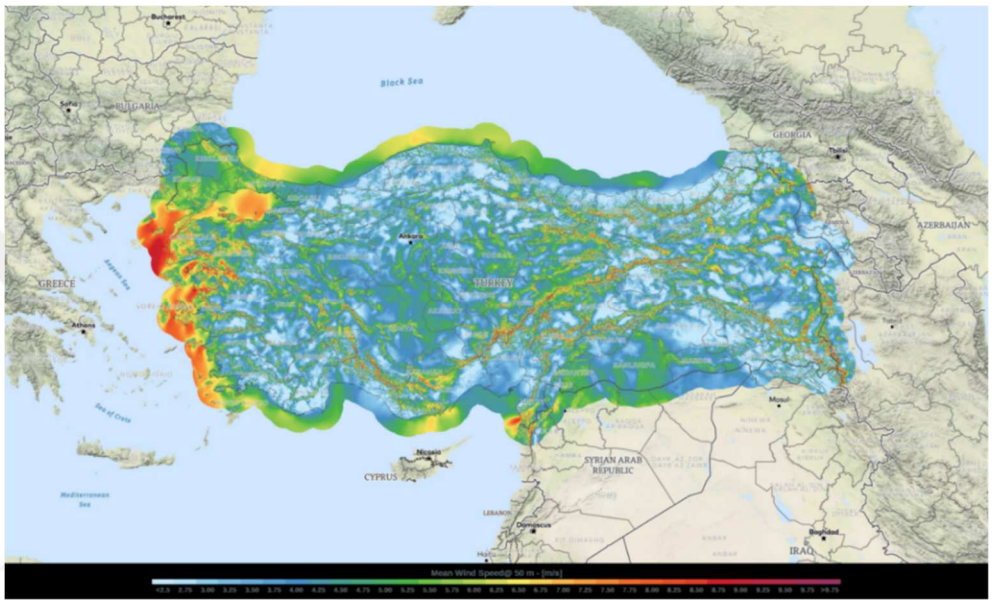

Figure 1.4 : Annual average wind speed map of Turkey (at 50 m).

- The most suitable areas for offshore wind are in the northwest of the Aegean Sea where wind speeds are up to 9 m/s.
- The Marmara Sea and the Black Sea have good wind speeds of 7 - 8 m/s.
- There are many opportunities on the west coast.
- The areas with water depth of less than 50 m have an offshore wind energy potential of 12 GW for bottom-fixed foundations.

2. OFFSHORE WIND TURBINES

2.1 Components of Offshore Wind Turbines

OWT is a wind turbine with support structure, subject to hydrodynamic loading (waves, extreme waves, and currents). OWT technologies are based on a three-bladed upwind horizontal axis design, although new concepts have been developed. As of now, all commercial OWTs are supported by the seabed. There are some variable floating supports under consideration. According to the International Electrotechnical Commission (IEC), the components of an OWT are shown in Figure 2.1. The IEC 61400-3 (Design Requirements for OWTs) design standard complements the IEC 61400-1 (Safety Requirements) design standard, specifies the design requirements for land-based wind turbines and design requirements for bottom-fixed OWTs.

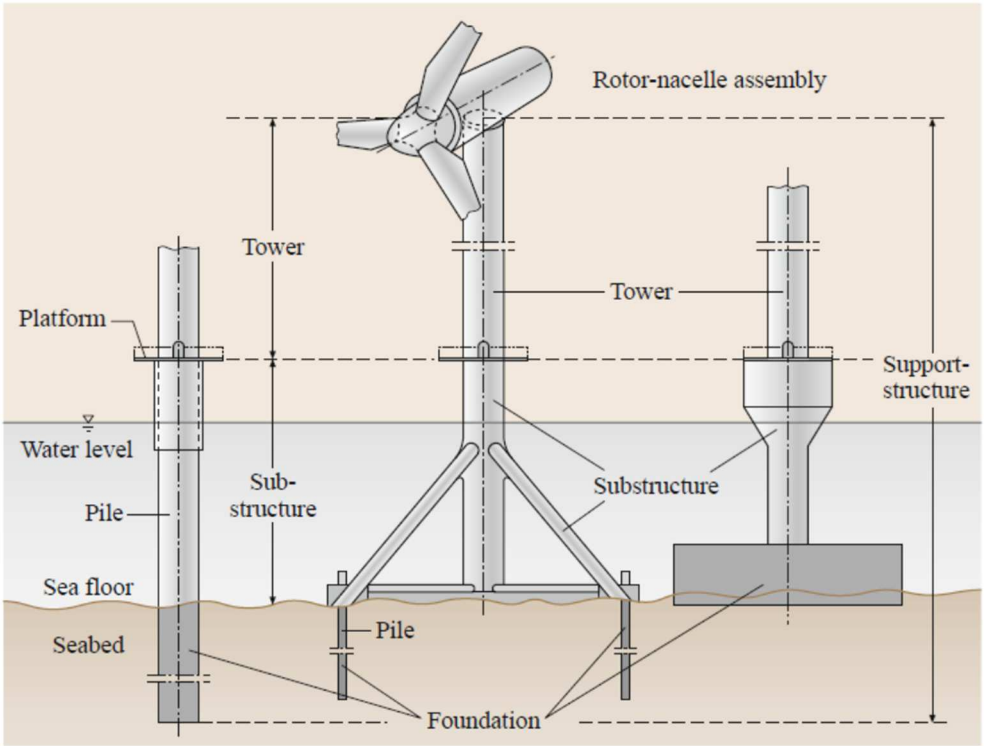

Figure 2.1 : Components of an offshore wind turbine.

OWTs consist of two main subsystems: the rotor-nacelle assembly (RNA) and the support structure.

2.1.1 Rotor nacelle assembly

There are two main component groups and a number of auxiliary components in the RNA. The main groups are the rotor and the drivetrain. The rotor includes hub, blades and pitch controller. The drivetrain includes shafts, gearbox, generator and brake. Other components include bedplate, yaw drive, yaw motor, climate controller, anemometer, wind vane and other electrical system components (shown in Figure 2.2).

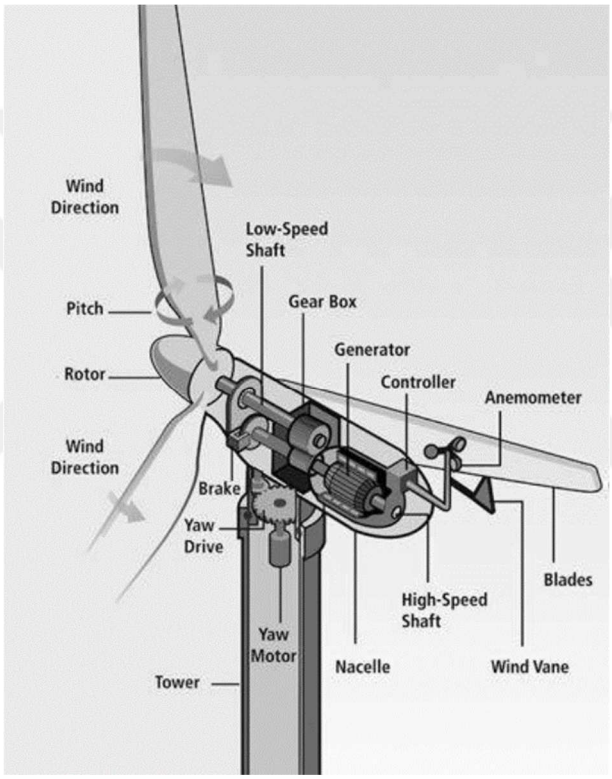

Figure 2.2 : Schematic of a typical wind turbine layout.

2.1.2 Support structure

2.1.2.1 Tower

The tower of an OWT is normally made of conical steel tubes. The tubes are made of different tower sections bolted together at the construction site to form a single structure of the desired height. The tower of an OWT is generally considered to end in a transition piece that is well above the waterline.

2.1.2.2 Substructure and foundation

The substructure is the rest of the support structure under the tower for the bottom-fixed OWTs; the foundation is actually the lower part of the substructure. Since the substructure and foundation cannot be uniquely separated for all configurations, they are defined together.

While land-based wind turbines require large concrete foundation structures, OWTs require different types of foundation structures depending on the water depth and material of the seabed. Foundation structures for OWTs include mono-pile, tri-pile, jacket, tri-pod, concrete gravity-based and floating support. Examples of foundation types for OWTs are shown in the Figure 2.3. They differ in their appearance, how loads are transferred to the soil, the way they are fixed to the seabed, and the water depths where they can be installed.

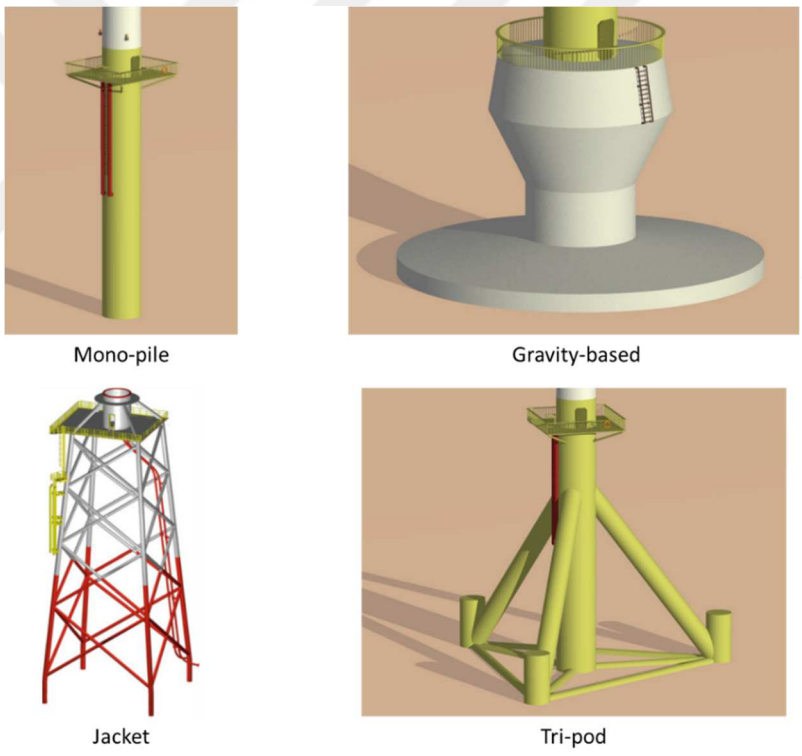

Figure 2.3 : Foundation types for offshore wind turbines.

Most of the offshore wind projects installed today use mono-pile or gravity-based foundations designed for shallow waters. Floating support foundations for deeper waters are also under development, but still not competitive.

3. EXTERNAL DESIGN CONDITIONS

The design of an OWF is highly dependent on the external conditions. Compared to an onshore wind farm, the many external conditions are considered for the design, operation and maintenance of an OWF. The main external design conditions in an OWF are wind, waves, soil conditions, and currents.

3.1 Wind

Wind is the most important external design condition in an OWF. Wind as the source determines the amount of energy produced. One of the important properties of wind is its temporal variability and includes:

- Short duration (turbulence and gusts),
- More or less short duration (hour to hour averages),
- Diurnal (changes within a day),
- Seasonal,
- Inter-yearly (from year to year).

Wind can also change spatially, both from one place to another and with its height above the ground. The Weibull distribution statistical model can be used to model the occurrences of wind speed. The probability density function (pdf) of the Weibull distribution is given by:

$$p(U) = \left(\frac{K}{C}\right)\left(\frac{U}{C}\right)^{K-1} exp\left[-\left(\frac{U}{C}\right)^{K}\right] \tag{3.1}$$

where K is the Weibull shape parameter and C is the Weibull scale parameter.

3.1.1 Wind power

The energy of an air particle per unit mass is simply given as half times the square of the wind speed. Mass flow rate of air passing through a specific area *A* perpendicular to the wind direction:

$$\dot{m} = \rho_a \, A \, U \tag{3.2}$$

where ρ_a is the air density of the standard atmosphere at sea level (= 1.225 kg/m^3 at 15°C temperature). Wind power per unit area:

$$\frac{P}{A} = \left(\frac{\dot{m}}{A}\right) \frac{1}{2} \, U^2 = \frac{1}{2} \, \rho_a \, U^3 \tag{3.3}$$

3.1.2 Wind shear

Wind shear is related to both turbine design and power generation. Wind shear is the change in wind speed with height. The estimated wind speed at height *h* is modeled with a log law as follows:

$$U_h = U_{ref} \left[\frac{ln\left(\frac{h}{z_0}\right)}{ln\left(\frac{h_{ref}}{z_0}\right)} \right] \tag{3.4}$$

where z_0 is the roughness length. For offshore, the range of roughness length is about 0.2 mm to 0.5 mm or more.

3.2 Waves

Waves have a very significant impact on the design of an OWF. Waves in the sea are formed primarily by the effect of wind. The higher the wind speed and the greater the distance over the sea it is moving, the higher the waves.

3.2.1 Regular waves

Regular waves are also known as “Airy waves”. Airy's model provides a useful starting point for discussing more complex wave behaviors. According to the Airy model, which includes a number of assumptions, a wave can be modeled as a sinusoid (shown in Figure 3.1).

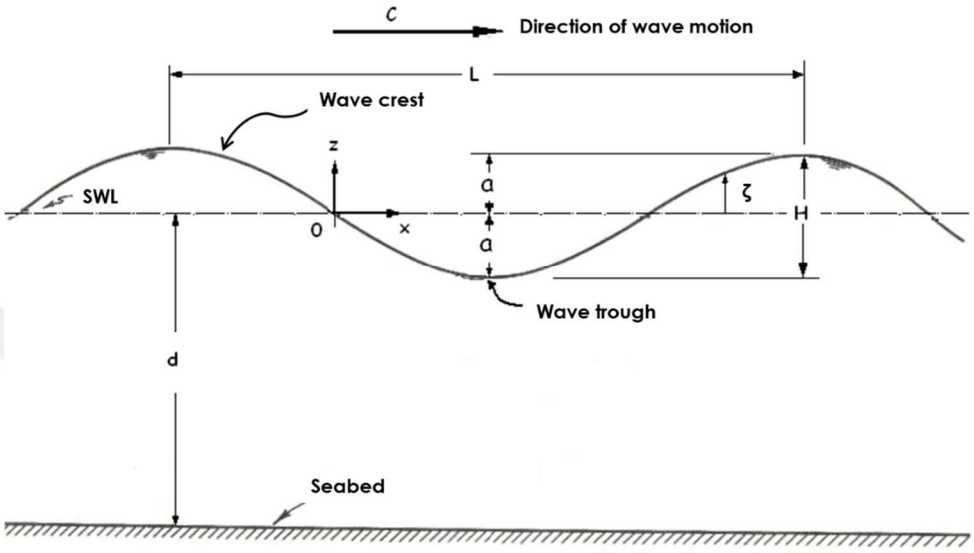

Figure 3.1 : Anatomy of a progressive sinusoidal wave.

The Airy wave profile (in the positive x-direction) is defined as:

$$\zeta(x,t) = a\,cos(k\,x - \omega\,t) \tag{3.5}$$

where *a* is the wave amplitude.

$H = 2\,a$ is the wave height.

$k = \frac{2\,\pi}{L}$ is the wave number, where *L* is the wavelength.

$\omega = \frac{2\,\pi}{T}$ is the circular frequency, where *T* is the wave period.

$c = \frac{\omega}{k} = \frac{L}{T}$ is the wave celerity (speed).

d is the water depth.

The water particles move in circular orbits with radius ζe^{kz}, where z is the distance up from the still water level (SWL).

The wavelength is expressed in terms of the wave period and the water depth by the following equation:

$$L = \frac{g\,T^2}{2\,\pi} tanh\left(\frac{2\,\pi\,d}{L}\right) \tag{3.6}$$

3.2.2 Empirical formulas for predicting waves

Making wave predictions is only possible if the geometry of the waterbody is relatively simple and the wave conditions are either fetch-limited or duration-limited. In most cases, the wave growth pattern at a site is a combination of the two cases.

The wave growth formulas are expressed in terms of adjusted wind speed (representing a relatively constant average value over the fetch). After the appropriate wind speed conversions are made, the wind speed is converted to an adjusted wind speed with the following formulas:

$$t = \frac{1609}{U_f} \tag{3.7}$$

where t is the time to travel 1 mile, U_f is the fastest mile wind speed.

$$\frac{U_f}{U_{3600}} = 1.277 + 0.296\ tanh\left[0.9\ log\left(\frac{45}{t}\right)\right] \tag{3.8}$$

where U_{3600} is the 1-hour average wind speed.

$$U_A = 0.71\ U^{1.23} \tag{3.9}$$

where U_A is the adjusted wind speed, $U = U_{3600}$.

In the fetch-limited case, the fetch (F) and the adjusted wind speed are the required parameters. The significant wave height (H_s) and the significant wave period (T_s) are the predicted parameters.

$$\frac{g\,H_s}{U^2} = 0.283\,tanh\left[0.0125\left(\frac{g\,F}{{U_A}^2}\right)^{0.42}\right] \tag{3.10}$$

$$\frac{g\,T_s}{2\,\pi\,U} = 1.2\,tanh\left[0.077\left(\frac{g\,F}{{U_A}^2}\right)^{0.25}\right] \tag{3.11}$$

3.2.3 Wave forces estimation

There are two main types of forces due to the waves:

1) Drag forces (related to the water velocity),
2) Inertia forces (related to the water acceleration).

The simplest equation that characterizes the forces on a structure due to waves is the Morison equation. For example, the force per unit length on a vertical cylinder of diameter D (shown in Figure 3.2) is as follows:

$$F = F_i + F_d = C_m\,\frac{1}{4}\,\rho\,\pi\,D^2\,\frac{du}{dt} + C_d\,\frac{1}{2}\,\rho\,D\,u\,|u| \tag{3.12}$$

where C_m is the inertia coefficient (about 2.0), C_d is the drag coefficient (typically between 0.5 and 1.5) and ρ is the seawater density (= 1025 kg/m^3).

If the restriction $\frac{D}{L} < 0.05$ satisfies, force calculations may be based on the equation (3.12).

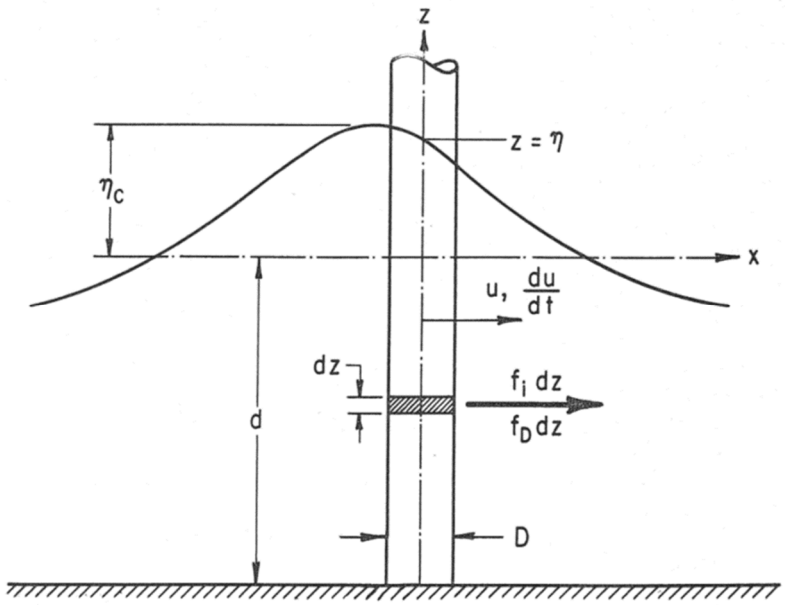

Figure 3.2 : Definition of wave forces on a vertical cylinder.

It should be noted that the Morison equation together with the Airy model can be used to find the total inertia and drag forces from waves on a vertical cylinder of diameter *D* (such as a mono-pile) in water of depth *d*. These:

$$F = \int_{-d}^{\zeta} f_i \, dz + \int_{-d}^{\zeta} f_D \, dz = -F_i \sin \omega t + F_d \cos^2 \omega t \qquad (3.13)$$

$$F_i = \frac{\pi}{4} \rho \, g \, C_m \, D^2 \, H \, K_i \qquad (3.14)$$

$$F_d = \frac{1}{2} \rho \, g \, C_d \, D \, H^2 \, K_d \qquad (3.15)$$

where

$$K_i = \frac{1}{2} tanh \, kd$$

$$K_d = \frac{1}{8}\left(1 + \frac{2kd}{sinh \, 2kd}\right)$$

The inertia and drag moments at the seabed can also be found as follows:

$$M = \int_{-d}^{\zeta} (z+d)\, f_i\, dz + \int_{-d}^{\zeta} (z+d)\, f_D\, dz = -M_i \sin \omega t + M_d \cos^2 \omega t \qquad (3.16)$$

$$M_i = d\, F_i\, S_i \qquad (3.17)$$

$$M_d = d\, F_d\, S_d \qquad (3.18)$$

where

$$S_i = 1 + \frac{(1 - \cosh kd)}{kd \sinh kd}$$

$$S_d = \frac{1}{2} + \frac{1}{8K_d}\left[\frac{1}{2} + \frac{(1 - \cosh 2kd)}{2kd \sinh 2kd}\right]$$

The inertia and drag forces do not reach their maximum simultaneously. The maximum occurs at $dF / dt = 0$, gives:

$dF / dt = -\omega F_i \cos \omega t - 2\, \omega F_d \cos \omega t \sin \omega t = -\omega (F_i + 2\, F_d \sin \omega t) \cos \omega t = 0$

In the first case ($F_i + 2\, F_d \sin \omega t = 0$), for maximum force:

$$\omega t = \theta_f = -\arcsin\left(\frac{F_i}{2F_d}\right) \quad \Longrightarrow \quad F_{max} = \left(\frac{{F_i}^2}{2F_d}\right) + F_d \cos^2 \theta_f \qquad (3.19)$$

By an identical process for maximum moment:

$$\omega t = \theta_m = -\arcsin\left(\frac{M_i}{2M_d}\right) \quad \Longrightarrow \quad M_{max} = \left(\frac{{M_i}^2}{2M_d}\right) + M_d \cos^2 \theta_m \qquad (3.20)$$

If $F_i / 2\, F_d > 1.0$ or $M_i / 2\, M_d > 1.0$, the above solutions become invalid. Then, the second case ($\cos \omega t = 0$) is used for obtaining the maximum, so that the resulting in:

$$\omega t = \theta_f = \theta_m = \frac{\pi}{2} \quad \Longrightarrow \quad F_{max} = -F_i \qquad M_{max} = -M_i \qquad (3.21)$$

3.3 Soil Conditions

Soil conditions are also important for the design of an OWF. Soil conditions affect the foundation and the electrical system. Soil conditions are closely related to the geology of the area. Therefore, the general properties of the soil can be evaluated depending on the location.

3.4 Currents

Currents can be of two types, wind-driven currents or tidal currents. Wind-driven currents are not a design factor, but can cause scours (removal of seabed soil) problem around the foundations (shown in Figure 3.3). Tidal currents can be very strong and add big loads to the foundations.

Figure 3.3 : Scour around the mono-pile foundation.

3.5 Environmental Impacts

OWTs are only responsible for pollution generation during their construction and do not emit any greenhouse gases or other pollutants (such as SO_x or NO_x) during operation. Environmental interaction with the marine life takes place where an OWF is located. It is possible that OWF and its infrastructure will affect the ecosystem in the area. Although there does not appear to be a direct danger to the marine life, the routes of fish and marine mammals may be affected and there is a possibility of deterioration of the entire ecosystem. The direct danger is only apparent for migratory birds that periodically cross the same routes.

In any real OWF project, the following issues may need to be explored:

- Noise impact,
- Barriers of water flow,
- Visual impact,
- Impacts on radio signals,
- Impacts on birds,
- Impacts on marine life,
- Impacts on benthic fauna and flora,
- Possibility of ship collisions.

There will always be various impacts on the immediate environment in which an OWF will be installed. However, with careful planning and research, these environmental disturbances can be prevented.

4. DESIGN OF AN OFFSHORE WIND FARM

In this section, the "Horns Rev I wind farm", which is the first large-scale OWF in the world, located on the west coast of Denmark is used as the reference OWF. The lifecycle (estimated 25 years) of an OWF project consists of four stages:

- Design and planning,
- Construction and installation,
- Operation and maintenance,
- Decommissioning.

The design of an OWF process begins with a detailed assessment of the internal (size of wind farm, financing of project, potential locations) and the external (water depth, marine life, shipping routes, borders, grid connection, soil, restrictions) design conditions at the site of interest. The following are decided for the design of an OWF:

- A location for the wind farm,
- The size and layout of wind farm,
- The type, model and hub height of wind turbine,
- The type of foundation.

4.1 Location

Firstly, a suitable location must be determined. The site selected for the OWF is the southwestern shores of Dikili. The location of the OWF is opposite the Island of Karaada, which is located in the Bay of Narlidere, in the Gulf of Candarli as shown in Figure 4.1.

Figure 4.1 : Location of the offshore wind farm.

Dikili, which is located in the Aegean region of Turkey, is a district of Izmir province (shown in Figure 4.2). Economy in Dikili is based on agriculture. Tourism is also an important source of income for Dikili, which is a popular summer resort. As of 2020, Dikili has a total population of 45,217.

Figure 4.2 : Location of Dikili district in Izmir.

The minimum distance from the Dikili shores to the northwest corner of the OWF is 1.16 km and the coordinates of the OWF obtained from the Google Earth Pro are as shown in Figure 4.3.

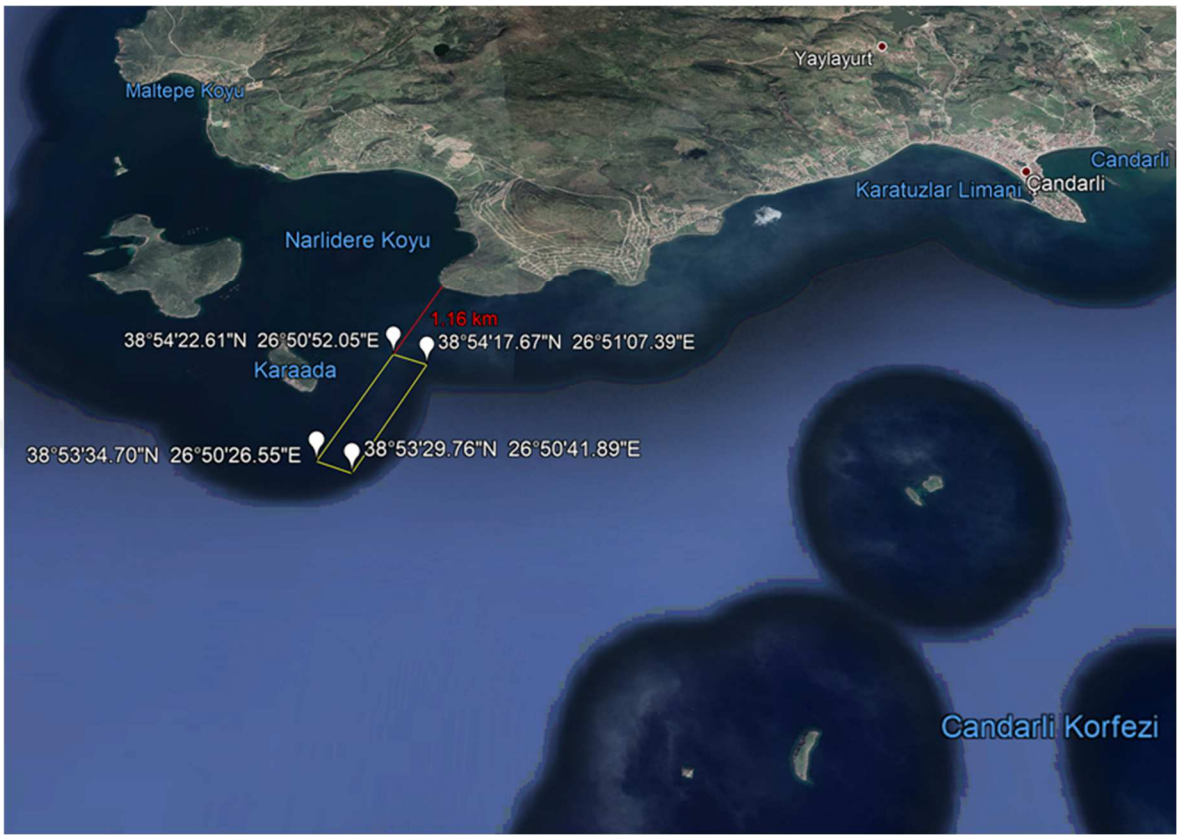

Figure 4.3 : Coordinates of the offshore wind farm.

The coordinates of the northwest corner of the OWF: 38°54'22.61"N 26°50'52.05"E

The coordinates of the northeast corner of the OWF: 38°54'17.67"N 26°51'07.39"E

The coordinates of the southwest corner of the OWF: 38°53'34.70"N 26°50'26.55"E

The coordinates of the southeast corner of the OWF: 38°53'29.76"N 26°50'41.89"E

4.1.1 Criteria for selecting location

4.1.1.1 Wind potential

Firstly, the wind speed at the selected location for an OWF should be within an acceptable range. Locations with wind speeds above 7 m/s (at 100 m hub height) are suitable for OWF installation. Accurate and reliable wind data are required for a better assessment of the selected location. The wind data should include wind speed, wind direction, temperature and humidity information.

Turkish State Meteorological Service is the government agency that provides wind data information only for onshore locations. There is no meteorological observation station in the seas of Turkey. The nearest meteorological observation station to the location of the OWF is Dikili Automatic Weather Station (AWS), whose the coordinates are 39°04'25.3"N 26°53'16.8"E (= 39.07°N 26.88°E) as shown in Figure 4.1. Dikili Automatic Weather Station is 19.7 km distance from the center of the OWF, whose the coordinates are 38°53'56.18"N 26°50'46.97"E (= 38.89°N 26.84°E). The nearest location to the center of the OWF is Karaada, whose the coordinates are 38.90°N 26.84°E. Therefore, the wind data of Karaada, which was obtained from the Meteoblue weather archive, is used for the OWF. The Meteoblue provides high-quality local weather information for any point in the world, whether on land or at sea. The Meteoblue climate diagrams are based on hourly weather model simulations. From 1985 to 2020, 35-year monthly weather archive diagrams for Karaada are given in Appendix A.

The dominant wind direction in Karaada is North-North-East (NNE), as shown in Figure 4.4. The wind rose for Karaada was obtained from the Meteoblue climate diagrams. It shows how many hours per year the wind (at 10 m height) blows from the indicated direction. NNE: Wind blows from NNE to South-South-West (SSW).

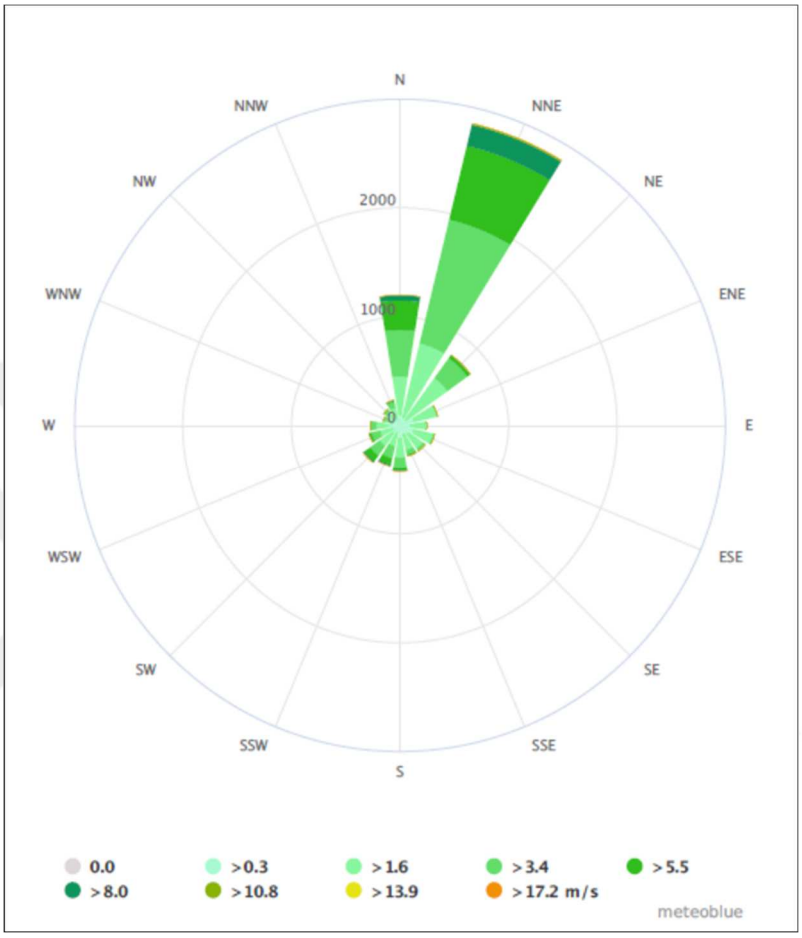

Figure 4.4 : Wind rose for Karaada (at 10 m).

The annual average wind speed is 8.75 m/s (at 50 m height) at the center of the OWF, as shown in Figure 4.5. The annual average wind speed map of the southern shores of Dikili was obtained from the GWA. This wind data information gives the best possible estimated of the wind energy potential of the OWF.

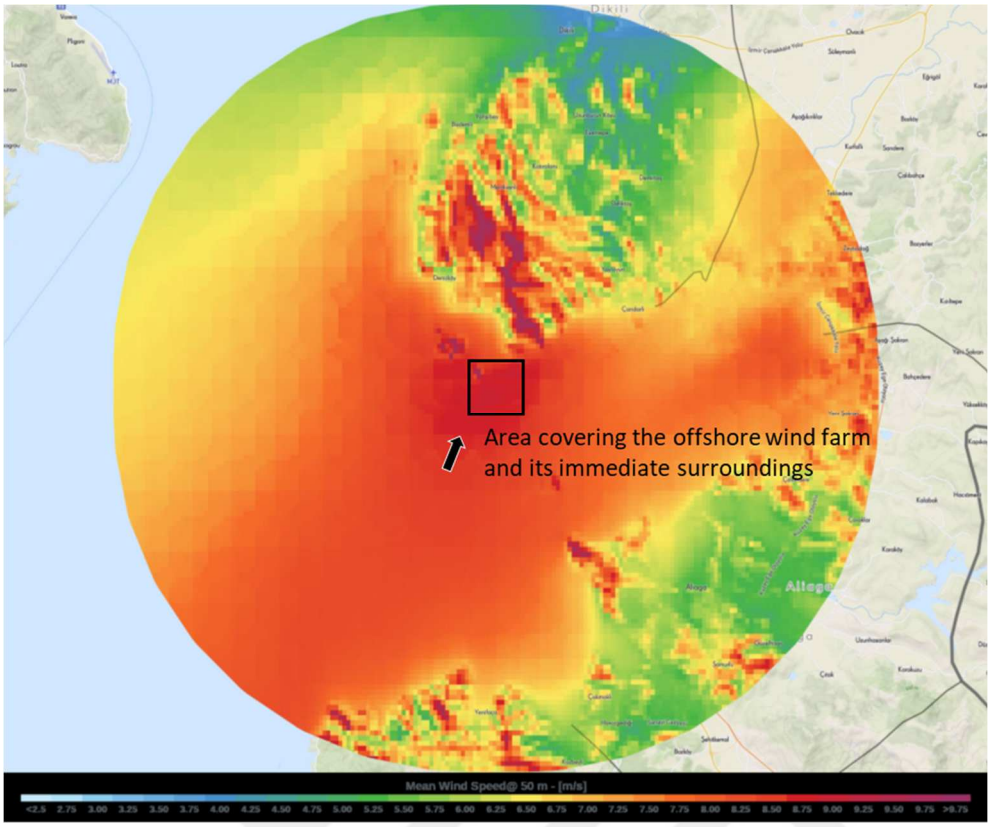

Figure 4.5 : Annual average wind speed map of the southern shores of Dikili.

The wind resource can be defined using an annual average wind speed and Weibull shape parameter. The wind speed Weibull distribution was obtained using the following characteristics for define the wind resource, as shown in Figure 4.6.

Annual average wind speed = 8.75 m/s

Reference height = 50 m

Weibull shape parameter = K = 2 (typical range is 1.5 - 2.5)

Weibull shape parameter is a parameter that reflects the width of distribution of wind speeds. Lower Weibull shape parameters correspond to broader wind speed distributions; this means that winds tend to vary over a wide range of speeds. Higher Weibull shape parameters correspond to narrower wind speed distributions; this means that wind speeds tend to stay in a narrow range.

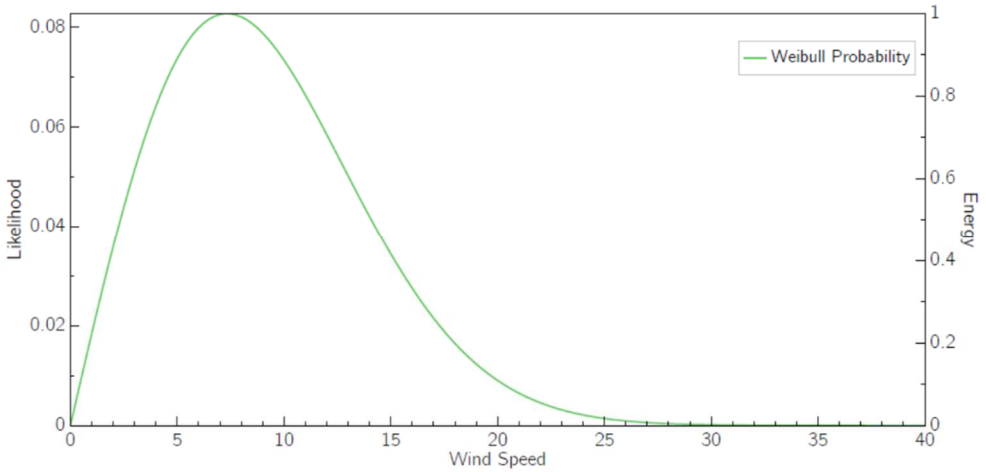

Figure 4.6 : Wind speed Weibull distribution for the offshore wind farm.

4.1.1.2 Territorial waters

There are many Greek islands, which is closer to Turkey, in the Aegean Sea as shown in Figure 4.7. The location of the OWF is in the territorial waters of Turkey. Thus, there is no problem with the national borders.

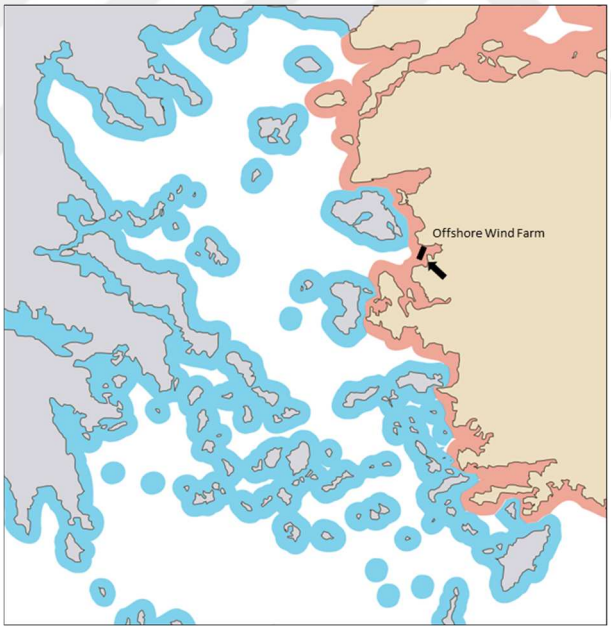

Figure 4.7 : Territorial waters in the Aegean Sea (based on 6 nmi).

4.1.1.3 Civil aviation

The selected location for an OWF should be away from airports. The location of the OWF is quite far from the nearest airport, Midilli International Airport, as shown in Figure 4.1.

4.1.1.4 Marine traffic

The selected location for an OWF should be away from heavy marine traffic. The location of the OWF is not on the shipping routes in the Aegean Sea.

4.1.1.5 Submarine pipelines and cable lines

The selected location for an OWF should not be on submarine pipelines and cable lines. There is no any submarine line at the location of the OWF.

4.2 Wind Farm Layout

The layout of wind turbines in a wind farm includes many considerations like turbine wake effects, ambient wind, available area, environmental restrictions, and visibility. The closer the turbines can be placed together, the lower the cost of the power cables in the wind farm. However, increased the turbulence and energy losses associated with turbine wakes can result in less power generation (depending upon topology, wind climate etc.) and higher maintenance cost. In offshore with respect to land, it can be larger turbine extension due to lower ambient turbulence and it can be larger turbine spacing (5 - 8 rotor diameters). The wind farm area consists of ten units OWT in two rows, with five wind turbines per row. The layout of wind turbines in the wind farm area is shown in Figure 4.8.

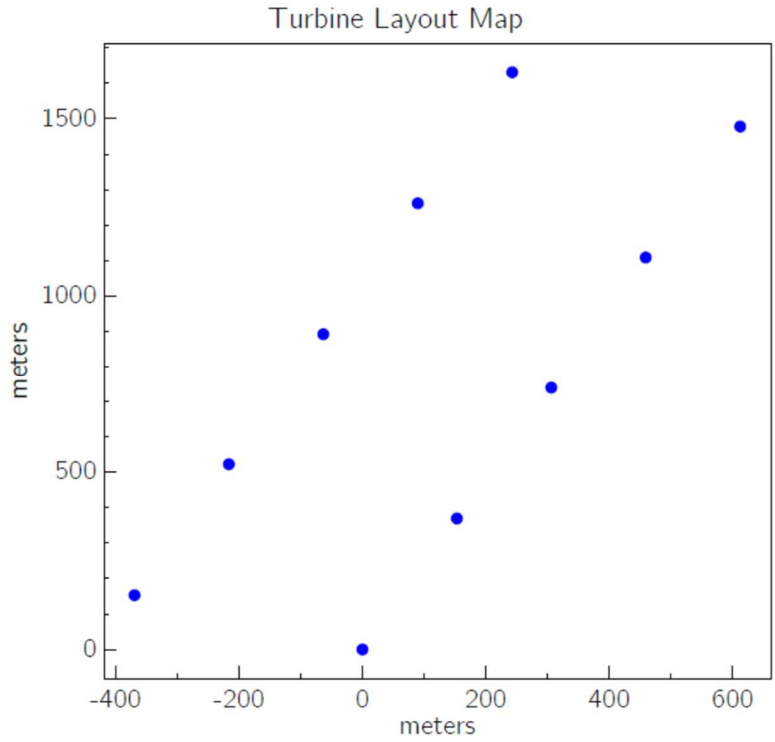

Figure 4.8 : Turbine layout map of the offshore wind farm.

Number of rows = 2 (in the NNE-SSW axis)

Turbines per row = 5 (facing the NNE direction)

Row spacing = 400 m (5 rotor diameters)

Turbine spacing = 400 m (5 rotor diameters)

Size of the wind farm (with 10 turbines) = 400 x 1600 m = 640,000 m^2

4.3 Wind Turbine

There are many OWT manufacturers on the market. Siemens Gamesa Renewable Energy is the current market leader with 69% of the total installed OWTs. MHI Vestas Offshore Wind is the second turbine manufacturer with 24%, followed by Senvion with 5%. These three manufacturers represent 98% of the all OWTs installed in Europe at the end of 2018.

The selected wind turbine for the OWF is “Vestas V80 - 2.0 Offshore” (78 m hub height). Its image is shown in Figure 4.9, and its power curve is shown in Figure 4.10. Its parameters are also given in Table 4.1. The wind turbine V80-2.0 Offshore is a production of Vestas Wind Systems A/S, a Danish manufacturer has been operating since 1979.

Figure 4.9 : Vestas V80 - 2.0 Offshore wind turbines in the North Hoyle wind farm.

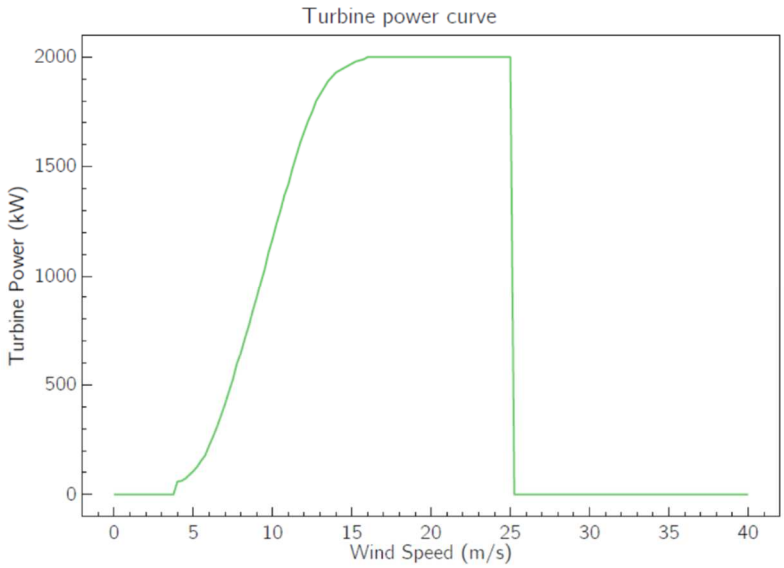

Figure 4.10 : Turbine power curve for Vestas V80 - 2.0 Offshore.

Table 4.1 : Vestas V80 - 2.0 Offshore wind turbine parameters.

Rotor	Diameter:	80 m	
	Area swept:	5027 m^2	
	Nominal revolutions:	16.7 rpm	
	Operational interval:	9 - 19 rpm	
	Number of blades:	3	
	Power regulation:	Pitch	
	Air brake:	3 separate hydraulic pitch cylinders	
Tower	Hub height:	60 m, 67 m, 78 m, 100 m	
	Type:	Steel tube (corrosion protection painted)	
Operational data	Cut-in wind speed:	4 m/s	
	Nominal wind speed:	15 m/s	
	Cut-out wind speed:	25 m/s	
Generator	Type:	Asynchronous doubly fed	
	Nominal output:	2000 kW	
	Operational data:	50 Hz / 60 Hz, 690 V	
Gearbox	Type:	Planet/parallel axles	
Control	Type:	Remote monitoring	
Weight	Nacelle:	67 t	
	Rotor:	37 t	
	Towers:		
	Hub height:	IEC IA	IEC IIA
	60 m	130 t	120 t
	67 m	160 t	135 t
	78 m	205 t	190 t
	100 m	-	225 t

4.3.1 Estimated annual average wind speed at hub height

The wind profile is obtained as below by using the wind shear equation (3.4).

$$U(h) = U(h_{ref})\left[\frac{ln\left(\frac{h}{z_0}\right)}{ln\left(\frac{h_{ref}}{z_0}\right)}\right]$$

h_{ref} = 50 m

z_o = 0.0002 m

U (50) = 8.75 m/s

For hub height h = 78 m

$$U(78) = 8.75\left[\frac{ln\left(\frac{78}{0.0002}\right)}{ln\left(\frac{50}{0.0002}\right)}\right] = 9.063 \text{ m/s}$$

4.3.2 Wind turbine IEC class

The selected wind turbine IEC class is IIA, according to the annual average wind speed at the center of the OWF. The wind speed parameters of the selected wind turbine class are taken from the Wind Turbine Generator System (WTGS) classes to IEC 61400-1 and listed in below:

WTGS Class: II - Medium wind

Turbulence Intensity Category: A - Higher turbulence

I_{15} = 18%

α = 2

U_{ave} = 9.063 m/s

In any case, the turbulence intensity can be calculated by using the formula:

$$I_u = \frac{I_{15}\left(\alpha + \frac{15}{U_{ave}}\right)}{(\alpha + 1)} = \frac{0.18\left(2 + \frac{15}{9.063}\right)}{(2 + 1)} = 0.2193 = 21.93\%$$

4.3.3 Maximum power

The maximum power in the wind is obtained as below by using the equation (3.3).

$$P = \frac{1}{2}\,\rho_a\,U^3\,A\,C_P$$

A = 5027 m^2

U = 9.063 m/s

C_p is the power coefficient (efficiency)

The theoretical maximum value of $C_p \approx 0.59$ (Betz limit)

$$P_{max} = \frac{1}{2}\,1.225\,(9.063)^3\,5027\,0.59 = 1352.33\ \text{kW}$$

4.3.4 Estimated energy production

Installed power of the OWF = 10 x 2 MW = 20 MW

$T_{equivalent}$ / T_{year} is called the capacity factor (*cf*)

cf ≈ 0.35 - 0.45 for OWFs → *cf* = 0.4 (can be taken as the average value)

Yearly energy production (E) will be produced in an equivalent time ($T_{equivalent}$) operating at full power (P_{rated}): $E = P_{rated}$ x $T_{equivalent}$

Energy yield = number of hours per year x *installed power* x *cf*

Energy yield = 8760 20 0.4 = 70 GWh/year

The OWF will generate an estimated 70 GWh/year of electricity energy. As of 2019, according to the United States Energy Information Administration (EIA), total electricity consumption of Turkey is 251,376 GWh/year and average electrical energy per capita is 3013 kWh/year.

4.3.5 Grid connection

The selected grid connection point is the Port of Narlidere, which is the nearest convenient place to the OWF, because power cables and their laying are costly. The maximum distance of the OWF from the Bay of Narlidere shores is 4.83 km. The distance to shore is very small therefore, there is no need to the OWTs are connected to an offshore substation. Substations are costly and brings (some) extra failure risks. The electricity generated by the OWTs can be transmitted directly to the shore and then integrated into the public grid. Grid connection topology for the OWTs is as shown in Figure 4.11. String topology is fairly simple and reliable power connection respect to looped topology. Generally, power cables in wind farms are relatively low voltage (24 to 36 kV). Therefore, power collection and transmission voltages can be taken as 30 kV (the average value) in the OWF. The electrical system of the OWF is briefly given in Table 4.2.

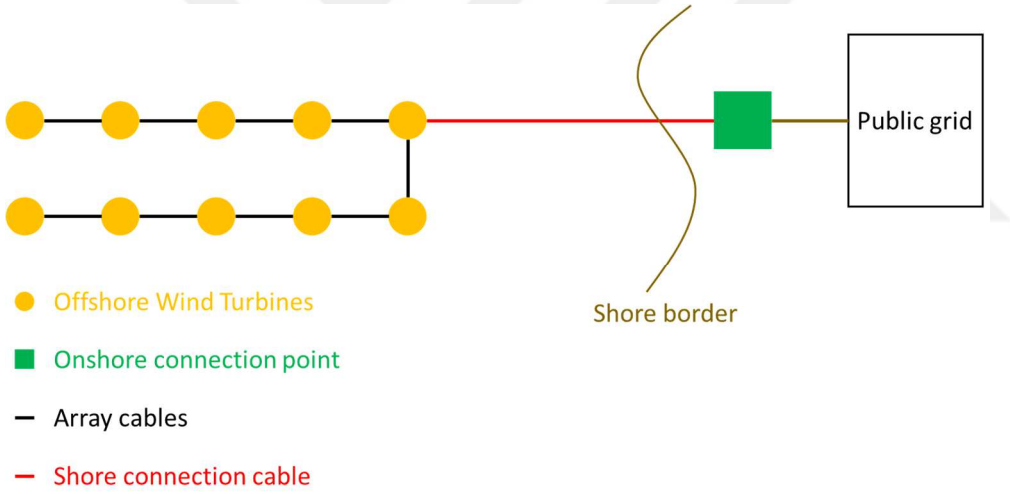

Figure 4.11 : Grid connection topology for the offshore wind turbines.

Table 4.2 : Electrical system of the offshore wind farm.

Installed power:	10 x 2 MW = 20 MW
Power collection voltage:	30 kV
Power transmission voltage:	30 kV
Distance to shore:	1.16 km
Shore connection:	AC connection on shore, wind farm voltage level
Network topology:	2 strings of 5 turbines

4.4 Substructure and Foundation

The selected foundation type for the OWF is mono-pile foundation. Design parameters of the mono-pile foundation system are also given in Table 4.3. The select of the foundation type is dependent on the water depth and the seabed conditions (soil type, scour). The maximum water depth at the location of the OWF is 25 m (as shown in Figure 4.12). The type of soil in the location of the OWF is mud (gravelly) as shown in Figure 4.13, which was obtained from the European Geological Data Infrastructure (EGDI).

Mono-pile foundations are proven technology, quite common and mainly used in shallow waters. They are represents 81.5% of all installed substructures in Europe at the end of 2018. They are usually economic and technically feasible for water depths less than 30 m. Suitable soil conditions for mono-piles are sand and silt layers, as they do not require pre-drilling.

Figure 4.12 : Bathymetry map of the southern shores of Dikili.

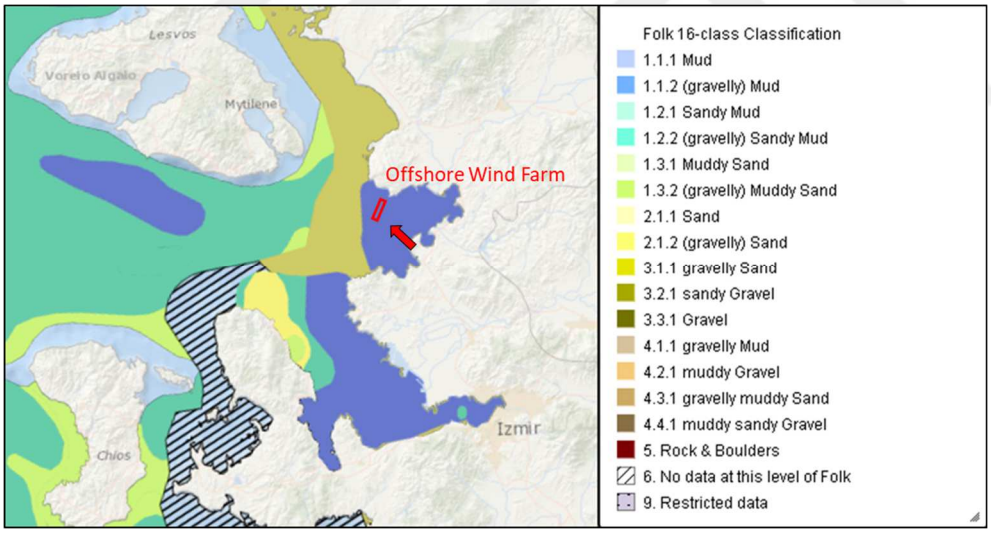

Figure 4.13 : Seabed substrate map of the Dikili shores.

A mono-pile consists of two main parts; a pile and a transition piece made of high quality steel. The pile is a cylindrical tube driven into the ground using a hydraulic hammer. The transition piece is the top on that the tower is bolted. The transition piece is equipped with work platform, intermediate platform, boat landing, navigation lights etc. The transition piece is connected to the pile by a grouting system. Schematic diagram of a mono-pile foundation system is shown in Figure 4.14.

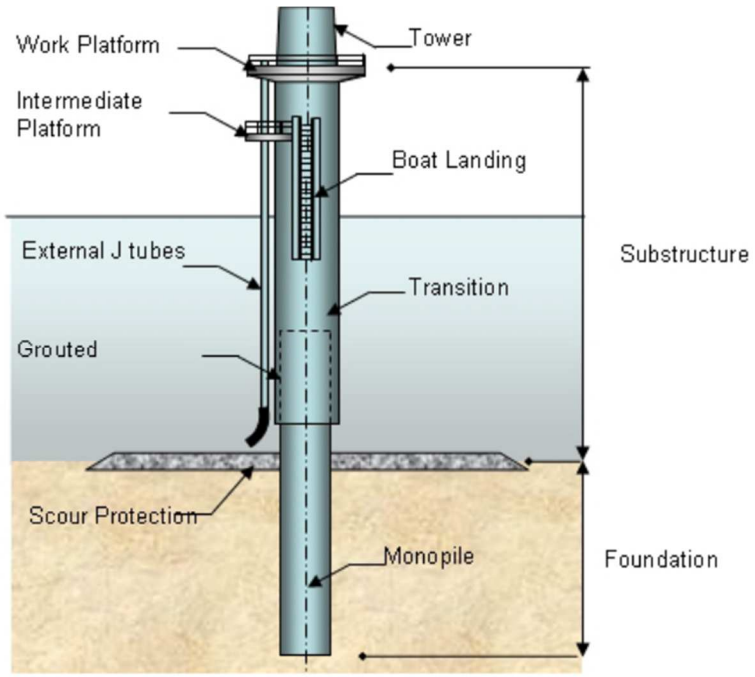

Figure 4.14 : Schematic diagram of a mono-pile foundation system.

Table 4.3 : Design parameters of the mono-pile foundation system.

The pile diameter (*D*) is 4 m and the wall thickness is 50 mm.
The effective fixity length (6*D* for general calculations) is 24 m (seabed penetration).
The transition piece diameter is 4.6 m and the grout is 6 m.
The working platform is 9 m above the sea level.
Two layers of stones (gravel) are used for the scour protection.

5. WAVE FORCES ESTIMATION

Wave forces must be considered in the design of an OWF. In this section, the maximum total wave force and moment acting on the mono-piles in the OWF were calculated using the Morison equation that can be useful for approximate results.

Maximum wind speeds that three different directions in the OWF (are given in Table 5.1) were determined from the monthly weather archive diagrams for Karaada (are given in Appendix A) and then they were obtained from the daily weather archive diagrams for Karaada (are given in Appendix B).

Table 5.1 : Maximum wind speeds and directions in the offshore wind farm.

Date	Wind speed (m/s)	Wind direction
February 22, 1993	20.3	South
March 9, 2011	21.7	North
December 31, 2014	24.7	North-East

The maximum water depth (25 m) in the OWF is at the southeast corner of the OWF. Therefore, three fetch distances in the directions of south, north and northeast from the southeast corner of the OWF are shown in Figure 5.1.

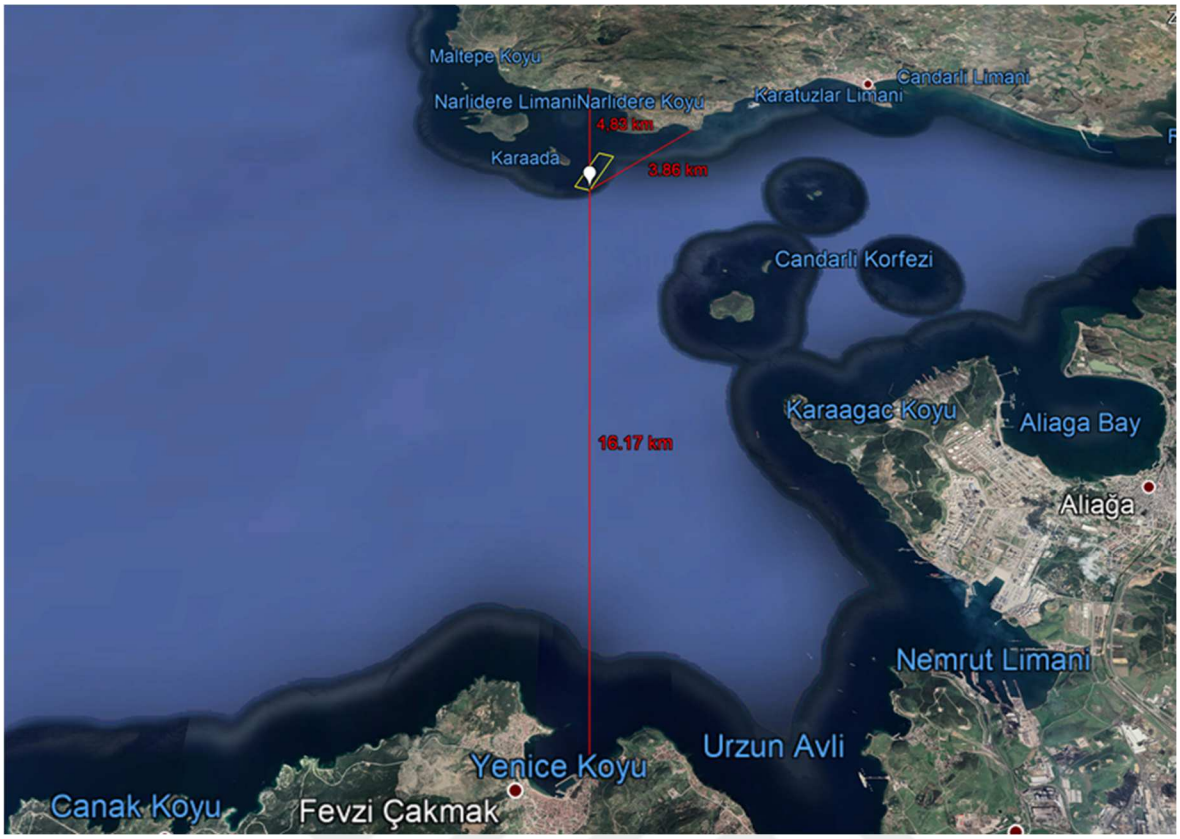

Figure 5.1 : Fetch distances from the southeast corner of the offshore wind farm.

5.1 Calculation of the Significant Wave Height and Significant Wave Period

The significant wave heights and the significant wave periods are obtained as below by using the equations from (3.7) to (3.11) for the maximum wind speed directions in the OWF.

For the direction of South: F = 16.17 km and U_f = 20.3 m/s

$$t = \frac{1609}{U_f} = \frac{1609}{20.3} = 79.261 \text{ s}$$

$$\frac{U_f}{U_{3600}} = 1.277 + 0.296\ tanh\left[0.9\ log\left(\frac{45}{t}\right)\right]$$

$$\frac{20.3}{U_{3600}} = 1.277 + 0.296\ tanh\left[0.9\ log\left(\frac{45}{79.261}\right)\right] \Rightarrow U_{3600} = 16.74 \text{ m/s} = U$$

$$U_A = 0.71\ U^{1.23} = 0.71(16.74)^{1.23} = 22.72 \text{ m/s}$$

$$\frac{g\,H_s}{U^2} = 0.283\,tanh\left[0.0125\left(\frac{g\,F}{{U_A}^2}\right)^{0.42}\right]$$

$$\frac{9.81\,H_s}{(16.74)^2} = 0.283\,tanh\left[0.0125\left(\frac{9.81\,16170}{(22.72)^2}\right)^{0.42}\right] \Rightarrow\ H_s = 1.11\ \text{m}$$

$$\frac{g\,T_s}{2\,\pi\,U} = 1.2\,tanh\left[0.077\left(\frac{g\,F}{{U_A}^2}\right)^{0.25}\right]$$

$$\frac{9.81\,T_s}{2\,3.14\,16.74} = 1.2\,tanh\left[0.077\left(\frac{9.81\,16170}{(22.72)^2}\right)^{0.25}\right] \Rightarrow\ T_s = 4.01\ \text{s}$$

For the direction of North: F = 4.83 km and U_f = 21.7 m/s

$$t = \frac{1609}{U_f} = \frac{1609}{21.7} = 74.147\ \text{s}$$

$$\frac{U_f}{U_{3600}} = 1.277 + 0.296\,tanh\left[0.9\,log\left(\frac{45}{t}\right)\right]$$

$$\frac{21.7}{U_{3600}} = 1.277 + 0.296\,tanh\left[0.9\,log\left(\frac{45}{74.147}\right)\right] \Rightarrow U_{3600} = 17.79\ \text{m/s} = U$$

$$U_A = 0.71\,U^{1.23} = 0.71(17.79)^{1.23} = 24.49\ \text{m/s}$$

$$\frac{g\,H_s}{U^2} = 0.283\,tanh\left[0.0125\left(\frac{g\,F}{{U_A}^2}\right)^{0.42}\right]$$

$$\frac{9.81\,H_s}{(17.79)^2} = 0.283\,tanh\left[0.0125\left(\frac{9.81\,4830}{(24.49)^2}\right)^{0.42}\right] \Rightarrow\ H_s = 0.71\ \text{m}$$

$$\frac{g\,T_s}{2\,\pi\,U} = 1.2\,tanh\left[0.077\left(\frac{g\,F}{{U_A}^2}\right)^{0.25}\right]$$

$$\frac{9.81\,T_s}{2\,3.14\,17.79} = 1.2\,tanh\left[0.077\left(\frac{9.81\,4830}{(24.49)^2}\right)^{0.25}\right] \Rightarrow\ T_s = 3.08\ \text{s}$$

For the direction of North-East: F = 3.86 km and U_f = 24.7 m/s

$$t = \frac{1609}{U_f} = \frac{1609}{24.7} = 65.142 \text{ s}$$

$$\frac{U_f}{U_{3600}} = 1.277 + 0.296\, tanh\left[0.9\, log\left(\frac{45}{t}\right)\right]$$

$$\frac{24.7}{U_{3600}} = 1.277 + 0.296\, tanh\left[0.9\, log\left(\frac{45}{65.142}\right)\right] \Rightarrow U_{3600} = 20.01 \text{ m/s} = U$$

$$U_A = 0.71\, U^{1.23} = 0.71(20.01)^{1.23} = 28.3 \text{ m/s}$$

$$\frac{g\, H_s}{U^2} = 0.283\, tanh\left[0.0125\left(\frac{g\, F}{{U_A}^2}\right)^{0.42}\right]$$

$$\frac{9.81\, H_s}{(20.01)^2} = 0.283\, tanh\left[0.0125\left(\frac{9.81\ 3860}{(28.3)^2}\right)^{0.42}\right] \Rightarrow H_s = 0.73 \text{ m}$$

$$\frac{g\, T_s}{2\, \pi\, U} = 1.2\, tanh\left[0.077\left(\frac{g\, F}{{U_A}^2}\right)^{0.25}\right]$$

$$\frac{9.81\, T_s}{2\ 3.14\ 20.01} = 1.2\, tanh\left[0.077\left(\frac{9.81\ 3860}{(28.3)^2}\right)^{0.25}\right] \Rightarrow T_s = 3.06 \text{ s}$$

Maximum values are taken from the calculations as the significant wave height (H_s) and the significant wave period (T_s).

$$H_s = 1.11\, m = H \quad and \quad T_s = 4.01\, m/s = T$$

5.2 Calculation of the Wave Forces and Wave Moments

The wavelength (L) is obtained as below by using the equation (3.6).

$$L_0 = \frac{g\,T^2}{2\,\pi} = \frac{9.81\,(4.01)^2}{2\;3.14} = 25.106 \text{ m}$$

$$d = 25 \text{ m}$$

$$L = L_0\,tanh\left(\frac{2\,\pi\,d}{L}\right) = 25.106\,tanh\left(\frac{2\;3.14\;25}{L}\right)$$

After several iterations $\Rightarrow\ L = 25.1$ m

$$\frac{d}{L} = \frac{25}{25.1} = 0.996 > 0.5 \ \Rightarrow \text{ Deep water wave}$$

$$k = \frac{2\,\pi}{L} = \frac{2\;3.14}{25.1} = 0.25 \text{ rad/m}$$

$$k\,d = 0.25\;25 = 6.25 \text{ rad}$$

$$2\,k\,d = 2\;0.25\;25 = 12.5 \text{ rad}$$

Hydrodynamic coefficients can be taken as $C_m \approx 2$ and $C_d \approx 0.7$.

The pile diameter can be taken as D = 1 m for the force calculations.

$$\frac{D}{L} = \frac{1}{25.1} = 0.04 < 0.05 \ \Rightarrow \text{ Therefore the equation (3.12) is valid.}$$

The inertia force (F_i) and the drag force (F_d) are obtained as below by using the equations (3.14) and (3.15).

$$K_i = \frac{1}{2}tanh\,k\,d = \frac{1}{2}tanh\,6.25 = 0.5$$

$$K_d = \frac{1}{8}\left(1 + \frac{2\,k\,d}{sinh\,2\,k\,d}\right) = \frac{1}{8}\left(1 + \frac{12.5}{sinh\,12.5}\right) = 0.125$$

$$F_i = \frac{\pi}{4}\,\rho\; g\; C_m\; D^2\; H\; K_i = \frac{\pi}{4}\; 1025\; 9.81\; 2\; 1^2\; 1.11\; 0.5 = 8766 \text{ N}$$

$$F_d = \frac{1}{2}\,\rho\; g\; C_d\; D\; H^2\; K_d = \frac{1}{2}\; 1025\; 9.81\; 0.7\; 1\; (1.11)^2\; 0.125 = 542 \text{ N}$$

The total wave force is obtained as below by using the equations (3.13) and (3.21).

$$F = -F_i\, sin\, \omega\, t + F_d\, cos^2\, \omega\, t$$

$$\frac{F_i}{2\, F_d} = \frac{8766}{2\; 542} = 8.1 > 1 \;\Rightarrow cos\, \omega\, t = 0 \;\Rightarrow\; \omega\, t = \frac{\pi}{2}$$

$$\omega\, t = \frac{\pi}{2}\; hence\; F_{max} = -F_i = -8766 \text{ N} *$$

The inertia moment (M_i) and the drag moment (M_d) are obtained as below by using the equations (3.17) and (3.18).

$$S_i = 1 + \frac{(1 - cosh\, k\; d)}{k\; d\;\; sinh\, k\; d} = 1 + \frac{(1 - cosh\, 6.25)}{6.25\;\; sinh\, 6.25} = 0.84$$

$$S_d = \frac{1}{2} + \frac{1}{8\; K_d}\left[\frac{1}{2} + \frac{(1 - cosh\, 2\; k\; d)}{2\; k\; d\;\; sinh\, 2\; k\; d}\right] = \frac{1}{2} + \frac{1}{8\; 0.125}\left[\frac{1}{2} + \frac{(1 - cosh\, 12.5)}{12.5\;\; sinh\, 12.5}\right] = 0.92$$

$$M_i = d\; F_i\; S_i = 25\; 8766\; 0.84 = 184{,}086 \text{ N. m}$$

$$M_d = d\; F_d\; S_d = 25\; 542\; 0.92 = 12{,}466 \text{ N. m}$$

Similarly, the total wave moment is obtained as below by using the equation (3.21).

$$\omega\, t = \frac{\pi}{2}\; hence\; M_{max} = -M_i = -184{,}086 \text{ N. m} *$$

$$\text{Effect point} \Rightarrow x_{max} = \frac{M_{max}}{F_{max}} = \frac{-184{,}086}{-8766} = 21 \text{ m (from the seabed)}$$

---

* The minus sign indicates the direction of force and moment and can be neglected when considering maximums.

6. CONCLUSIONS AND RECOMMENDATIONS

OWFs have some advantages. Offshore winds are stronger and more stable than onshore winds. Offshore winds are less turbulent than onshore winds. This increases its service life. The sea offers less resistance to wind flow, resulting in lower wind shear. Offshore wind projects can be considered more environmentally.

Turkey has a rapidly growing economy and thus increasing energy demand. A very large part of Turkey's energy demand is met by imported fossil fuels. Potential OWFs with together onshore wind farms can help to meet Turkey's increasing energy demand, and to limit its dependence on energy imports. In addition, OWFs that use only the wind to generate electrical power can also help to reduce greenhouse gas emissions of Turkey.

In this thesis, a potential OWF with size of 640,000 m^2 (400 x 1600 m) project was technically designed as a case study. The OWF is located opposite the Island of Karaada, which is located in the Bay of Narlidere, 1.16 km distance from the southwestern shores of Dikili. The annual average wind speed is 8.75 m/s (at 50 m height) at the center of the OWF. With strong and steady winds, this site is suitable location for the wind power generation. According to the research on the location, no potential obstacles in terms of environmental impacts were identified before the OWF project realization.

Installed power of the OWF is 20 MW. The ten units "Vestas V80 - 2.0 Offshore" model wind turbines with 78 m hub height and 80 m rotor diameter (in two rows with five turbines each facing the NNE direction) are installed in mud (gravelly) type soil at a maximum water depth of 25 m using the mono-pile foundation system.

The OWF will generate an estimated 70 GWh/year of electricity energy. This clean and sustainable electricity, which will be transmitted directly into the public grid from the OWF with the Port of Narlidere connection point, can meet the annual electricity needs of approximately 23,000 households. This is equal to about half of Dikili's population.

For the significant wave height (H_s) of 1.11 m and the significant wave period (T_s) of 4.01 m/s, the maximum total wave force (F_{max}) as −8766 N and the maximum total wave moment (M_{max}) as −184,086 N.m acting on the mono-piles in the OWF were calculated using the Morison equation. These approximate results can be useful during the development of the OWF.

In addition, an OWF project must be analyzed economically during the development phase. Accordingly, a feasibility study should be done before the OWF project is realized and the following costs should be calculated for the financing of the project.

- Project and license costs,
- Turbine costs,
- Electrical infrastructure costs,
- Installation costs,
- Transportation costs,
- Construction costs,
- Operation and maintenance costs.

REFERENCES

Akova, I. (2011). *Development Potential of Wind Energy in Turkey*, EchoGéo 16, Open edition Journals.

Argin, M. ve Yerci, V. (2015). *The Assessment of Offshore Wind Power Potential of Turkey*, Ninth International Conference on Electrical and Electronics Engineering (ELECO).

Barutçu, B. (2010). *Wind Energy and Conversion Technology*, EBT 527E Course Notes, Istanbul Technical University.

Burton T., Sharpe D., Jenkins N., Bossanyi E. (2001). *Wind Energy Handbook*, Wiley, Chichester.

Dalén, G. (2013). *Offshore Wind Power*, M. Kaltschmitt et al. (eds.), Renewable Energy Systems, Springer, New York.

Hau, E. (2013). *Wind Turbines: Fundamentals, Technologies, Application, Economics*, Third translated edition, Springer, Heidelberg.

IEC (International Electrotechnical Commission). (2009). *Wind Turbines-Part 3: Design Requirements for Offshore Wind Turbines, IEC 61400-3* Geneva.

Lützen, U. (2017). *Offshore Wind Farm Design*, ADM 507E Course Notes, Istanbul Technical University.

Manwell, J. F. (2013). *Offshore Wind Energy Technology Trends, Challenges, and Risks*, M. Kaltschmitt et al. (eds.), Renewable Energy Systems, Springer, New York.

MacDonald, M. (2010). *Schematic diagram of a monopile foundation system*, Offshore Wind - IEEE Boston PES.

Moan, T. (2015). *Recent Development of Analysis and Design of Offshore Wind Turbines for Deep Water,* Renewable Energies Offshore, C. Guedes Soares (Ed.), Taylor & Francis Group, London.

SAM (System Advisor Model). (2019). *Wind Speed Weibull Distribution, Turbine Power Curve, Turbine Layout Map*, SAM version 2018.11.11.

Sarpkaya, T. and Isaacson, M. (1981). *Mechanics of Wave Forces on Offshore Structures*, First edition, Van Nostrand Reinhold Company, New York.

Satir, M., Murphy, F., McDonnell, K. (2017). *Feasibility Study of an Offshore Wind Farm in the Aegean Sea, Turkey*, Renewable and Sustainable Energy Reviews.

Strach-Sonsalla, M., Stammler, M., Wenske, J., Jonkman, J., Vorpahl, F. (2016). *Offshore Wind Energy*, Ocean Renewable Energy-Part E/49.

Wind Europe. (2019). *Offshore Wind in Europe: Key Trends and Statistics 2018*, Wind Europe Annual Report, Brussels.

Url-1 < *https://www.aquaret.com/images/stories/aquaret/pdf/chapter5.pdf* >, date retrieved 12.10.2018.

Url-2 < *https://iea-retd.org/archives/publications/rewind-offshore* >, date retrieved 15.11.2018.

Url-3 < *https://tr.wikipedia.org/wiki/Dikili* >, date retrieved 17.07.2019.

Url-4 < *https://map.openseamap.org/Karaada* >, date retrieved 19.07.2019.

Url-5 < *https://en.wind-turbine-models.com/turbines/668-vestas-v80-offshore* >, date retrieved 29.10.2019.

Url-6 < *https://globalwindatlas.info/Dikili* >, date retrieved 04.01.2020.

Url-7 < *https://www.europe-geology.eu/marine-geology/seabed-substrate/* >, date retrieved 05.01.2020.

Url-8 < *https://www.worldbank.org/en/topic/energy/publication/expanding-offshore-wind-in-emerging-markets* >, date retrieved 28.01.2020.

Url-9 < *https://www.meteoblue.com/tr/hava/archive/export/karaada_türkiye_310395* >, date retrieved 10.02.2020.

Url-10 < *https://en.wikipedia.org/wiki/List_of_countries_by_electricity_consumption* >, date retrieved 24.04.2021.

APPENDICES

APPENDIX A: 35-year monthly weather archive diagrams for Karaada.

APPENDIX B: 3-month (months with maximum wind speeds) daily weather archive diagrams for Karaada.

APPENDIX A

The Meteoblue weather archive diagrams shows simulation data for the selected location. The diagrams show hourly data. There are monthly aggregations for minimum, maximum and average values over a year. The weather archive diagrams are divided into three charts:

1) Minimum, maximum and average temperature (orange lines), including relative humidity (blue line).
2) Precipitation amount (blue bars), clouds (gray background) and clear sky (yellow background).
3) Minimum, maximum and average wind speed (green lines) and wind direction (purple points) are specified in degrees: 0° = North, 90° = East, 180° = South, 270° = West.

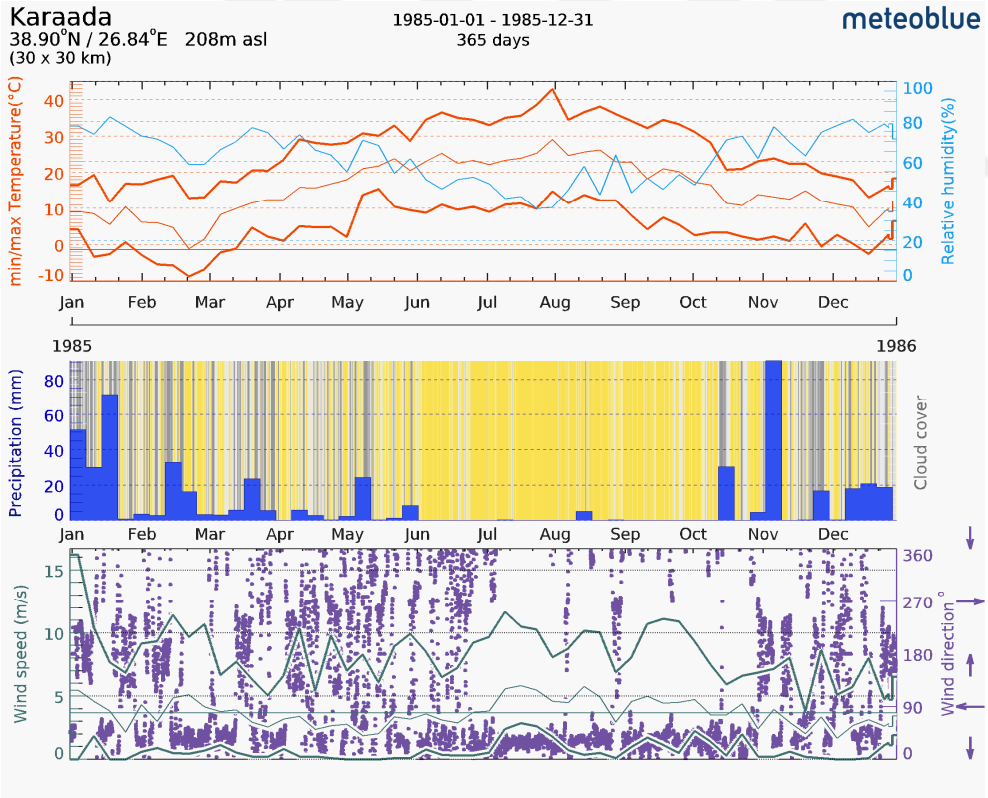

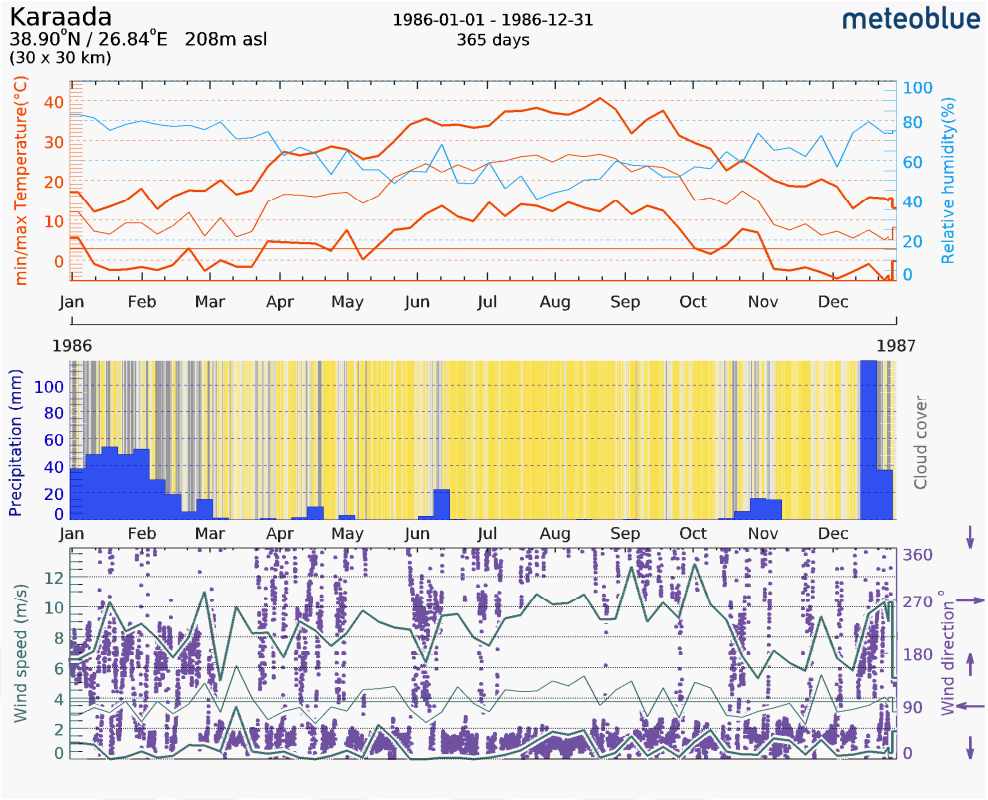
Karaada
38.90°N / 26.84°E 208m asl
(30 x 30 km)
1986-01-01 - 1986-12-31
365 days
meteoblue
min/max Temperature(°C)
Relative humidity(%)
Jan Feb Mar Apr May Jun Jul Aug Sep Oct Nov Dec
1986
1987
Precipitation (mm)
Cloud cover
Wind speed (m/s)
Wind direction °

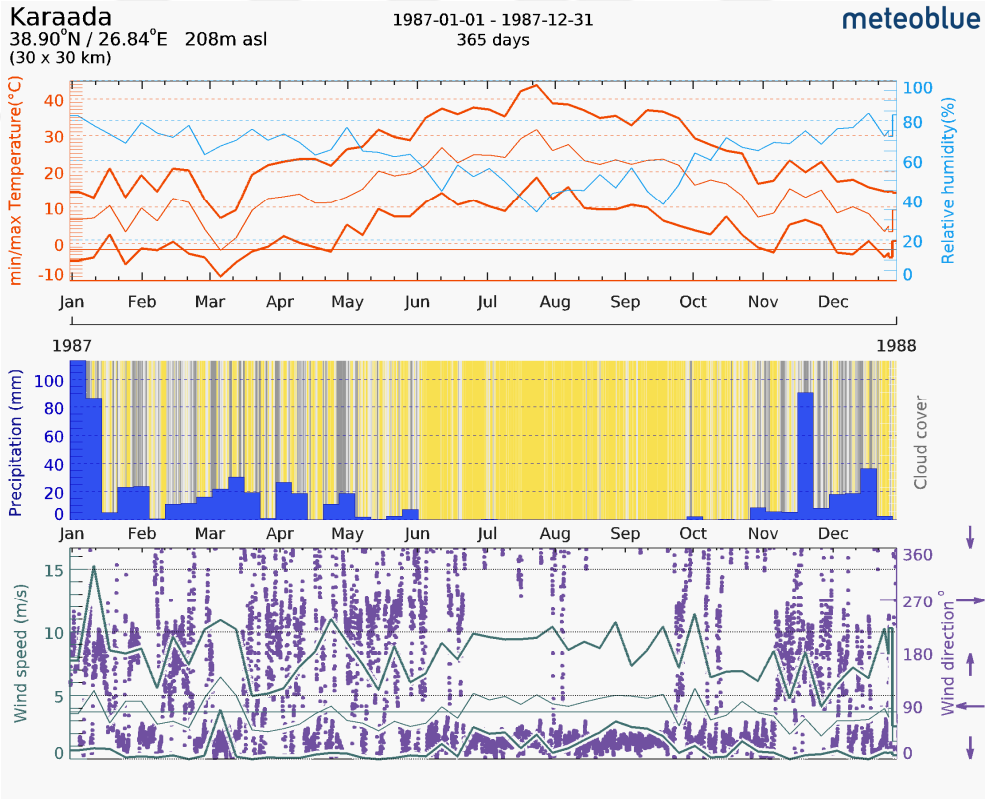
Karaada
38.90°N / 26.84°E 208m asl
(30 x 30 km)
1987-01-01 - 1987-12-31
365 days
meteoblue
min/max Temperature(°C)
Relative humidity(%)
Jan Feb Mar Apr May Jun Jul Aug Sep Oct Nov Dec
1987
1988
Precipitation (mm)
Cloud cover
Wind speed (m/s)
Wind direction °

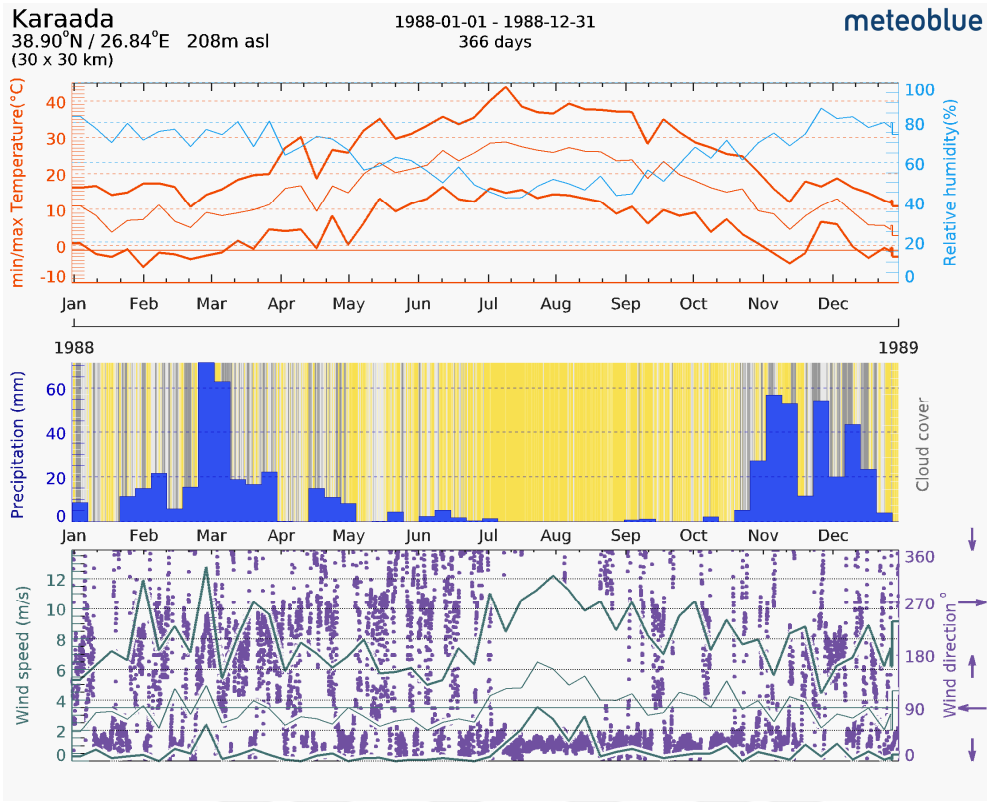
Karaada
38.90°N / 26.84°E 208m asl
(30 x 30 km)
1988-01-01 - 1988-12-31
366 days
meteoblue
min/max Temperature(°C)
Relative humidity(%)
Jan Feb Mar Apr May Jun Jul Aug Sep Oct Nov Dec
1988
1989
Precipitation (mm)
Cloud cover
Wind speed (m/s)
Wind direction °

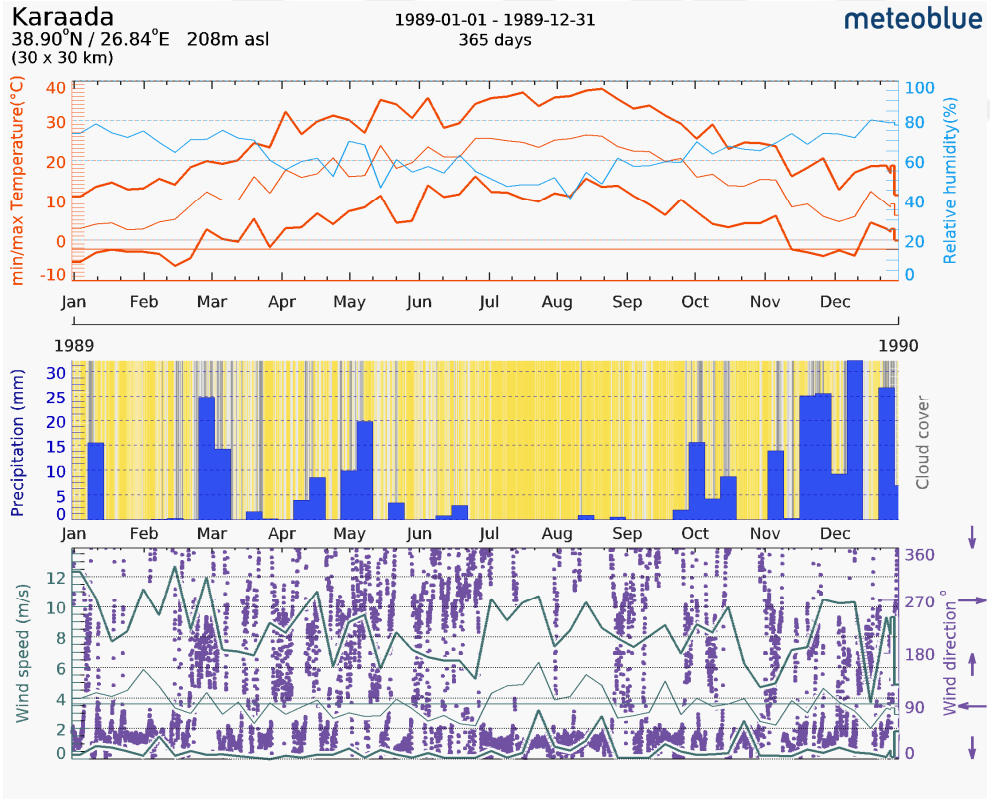
Karaada
38.90°N / 26.84°E 208m asl
(30 x 30 km)
1989-01-01 - 1989-12-31
365 days
meteoblue
min/max Temperature(°C)
Relative humidity(%)
Jan Feb Mar Apr May Jun Jul Aug Sep Oct Nov Dec
1989
1990
Precipitation (mm)
Cloud cover
Wind speed (m/s)
Wind direction °

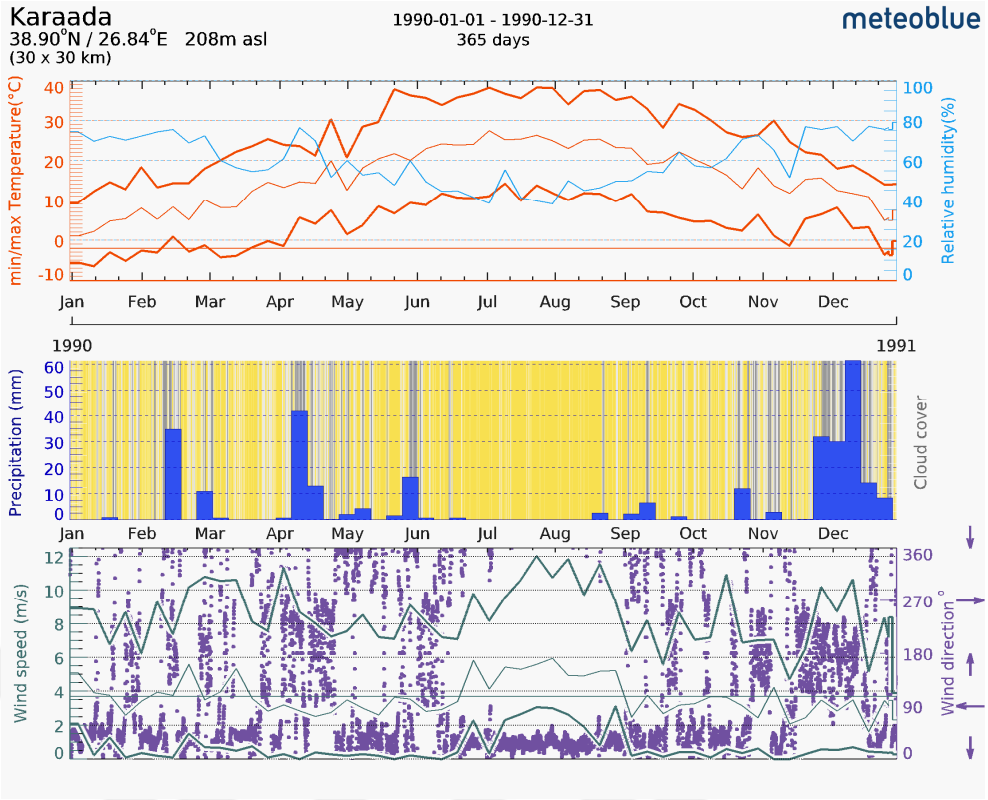
Karaada
38.90°N / 26.84°E 208m asl
(30 x 30 km)
1990-01-01 - 1990-12-31
365 days
meteoblue
min/max Temperature(°C)
Relative humidity(%)
Jan Feb Mar Apr May Jun Jul Aug Sep Oct Nov Dec
1990
1991
Precipitation (mm)
Cloud cover
Wind speed (m/s)
Wind direction °

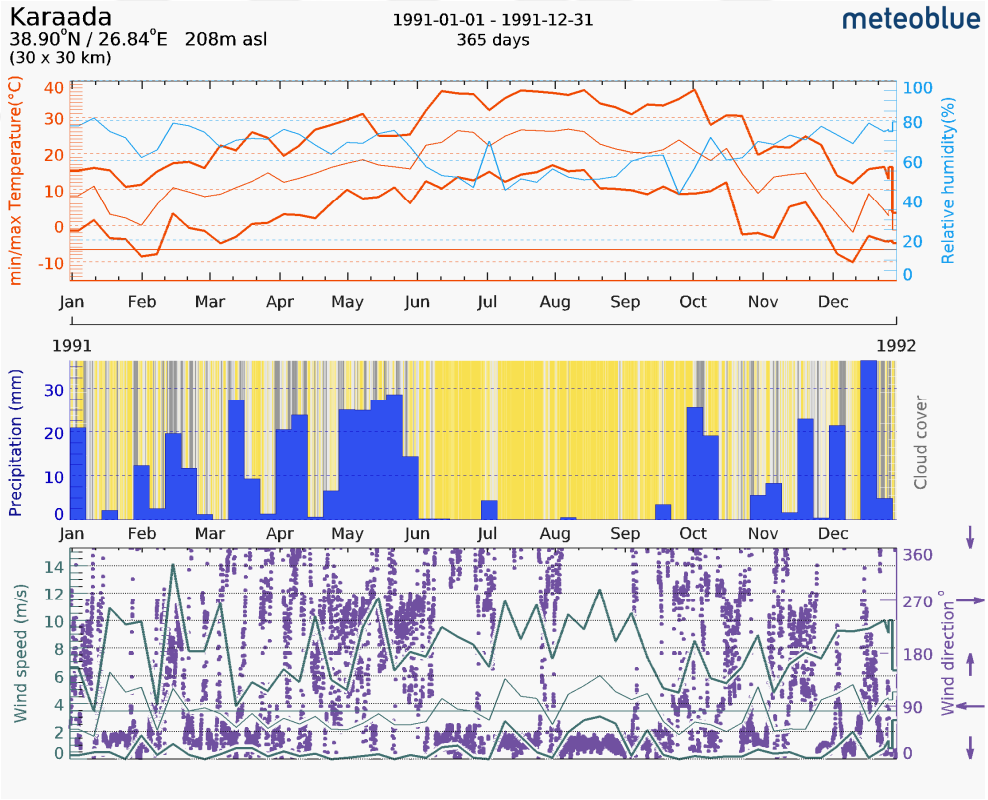
Karaada
38.90°N / 26.84°E 208m asl
(30 x 30 km)
1991-01-01 - 1991-12-31
365 days
meteoblue
min/max Temperature(°C)
Relative humidity(%)
Jan Feb Mar Apr May Jun Jul Aug Sep Oct Nov Dec
1991
1992
Precipitation (mm)
Cloud cover
Wind speed (m/s)
Wind direction °

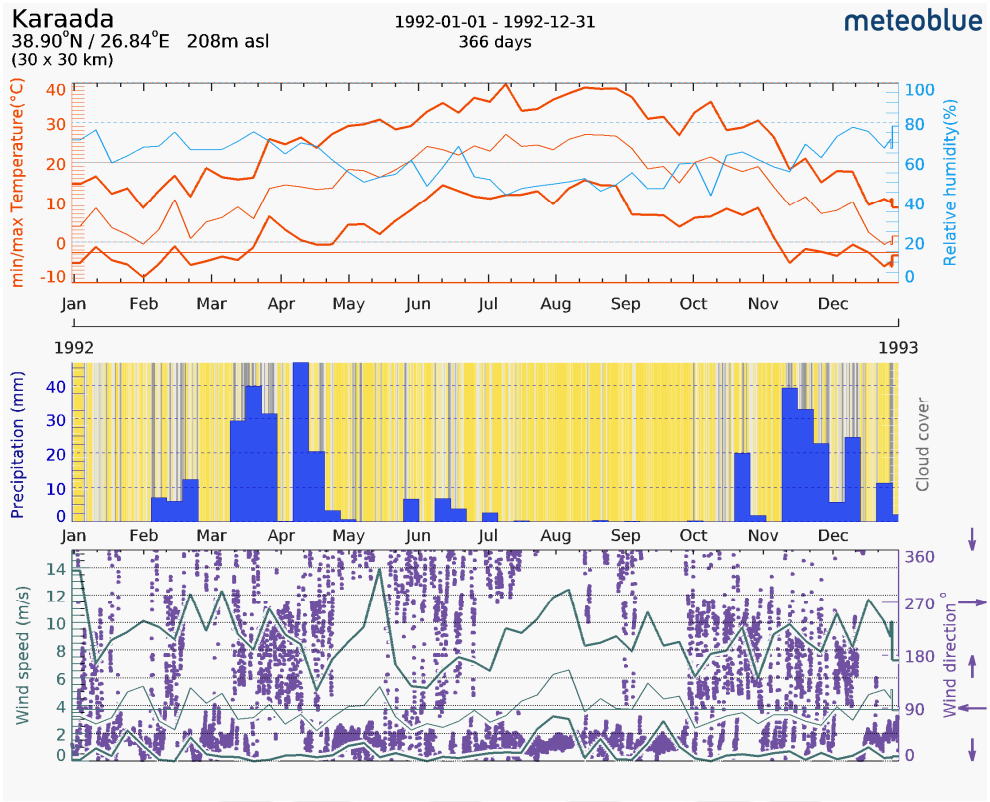
Karaada
38.90°N / 26.84°E 208m asl
(30 x 30 km)
1992-01-01 - 1992-12-31
366 days
meteoblue
min/max Temperature(°C)
Relative humidity(%)
Jan Feb Mar Apr May Jun Jul Aug Sep Oct Nov Dec
1992
1993
Precipitation (mm)
Cloud cover
Wind speed (m/s)
Wind direction °

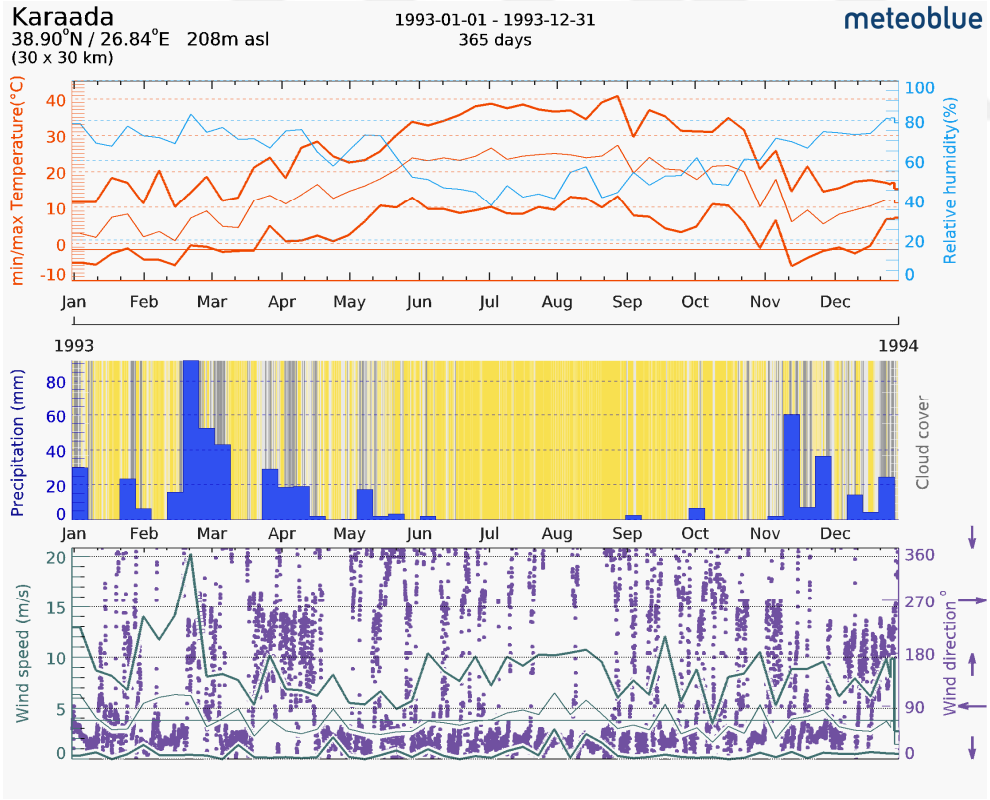
Karaada
38.90°N / 26.84°E 208m asl
(30 x 30 km)
1993-01-01 - 1993-12-31
365 days
meteoblue
min/max Temperature(°C)
Relative humidity(%)
Jan Feb Mar Apr May Jun Jul Aug Sep Oct Nov Dec
1993
1994
Precipitation (mm)
Cloud cover
Wind speed (m/s)
Wind direction °

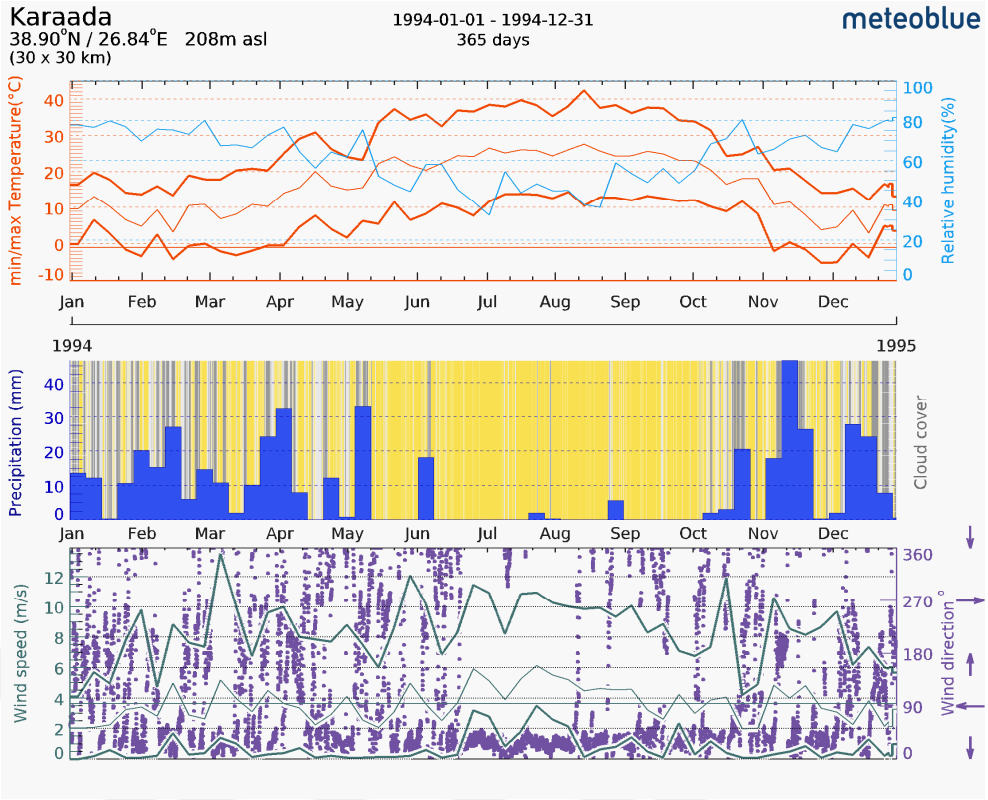
Karaada
38.90°N / 26.84°E 208m asl
(30 x 30 km)
1994-01-01 - 1994-12-31
365 days
meteoblue
min/max Temperature(°C)
Relative humidity(%)
Jan Feb Mar Apr May Jun Jul Aug Sep Oct Nov Dec
1994
1995
Precipitation (mm)
Cloud cover
Wind speed (m/s)
Wind direction °

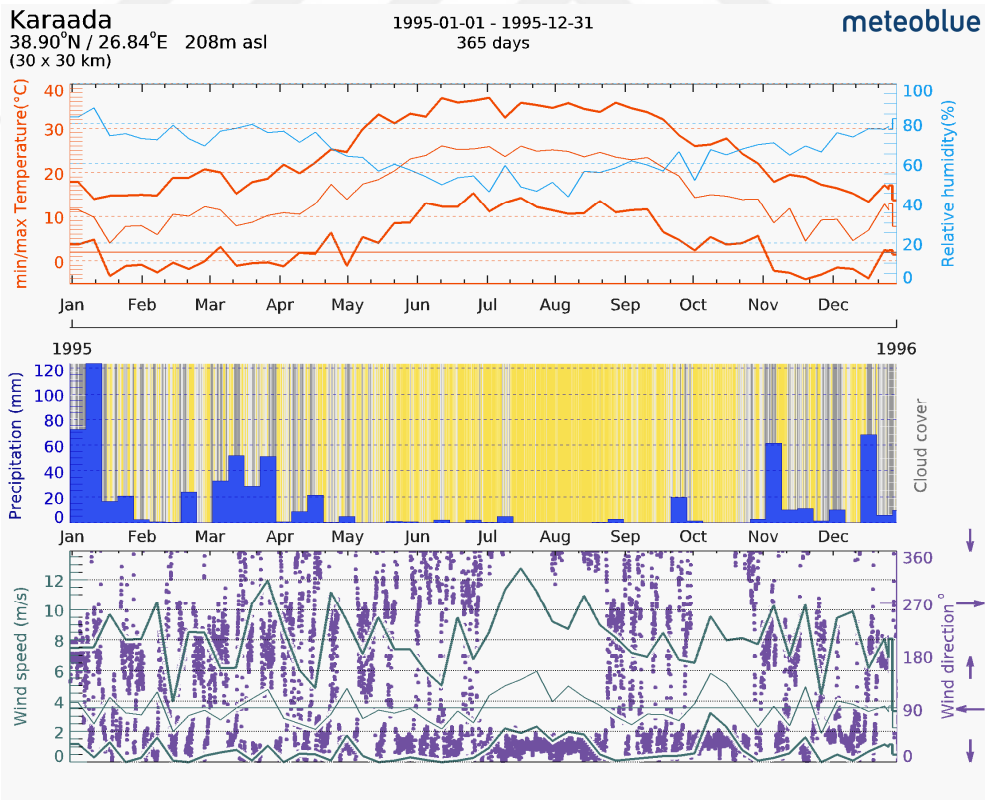
Karaada
38.90°N / 26.84°E 208m asl
(30 x 30 km)
1995-01-01 - 1995-12-31
365 days
meteoblue
min/max Temperature(°C)
Relative humidity(%)
Jan Feb Mar Apr May Jun Jul Aug Sep Oct Nov Dec
1995
1996
Precipitation (mm)
Cloud cover
Wind speed (m/s)
Wind direction °

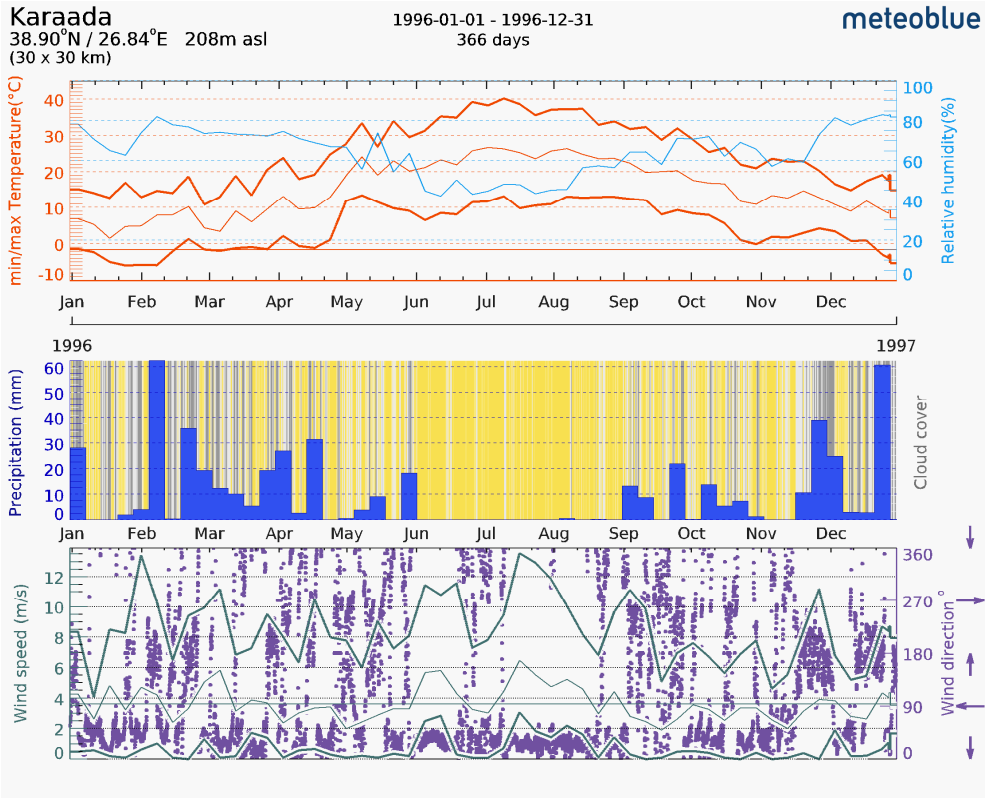
Karaada
38.90°N / 26.84°E 208m asl
(30 x 30 km)
1996-01-01 - 1996-12-31
366 days
meteoblue
min/max Temperature(°C)
Relative humidity(%)
Jan Feb Mar Apr May Jun Jul Aug Sep Oct Nov Dec
1996
1997
Precipitation (mm)
Cloud cover
Wind speed (m/s)
Wind direction °

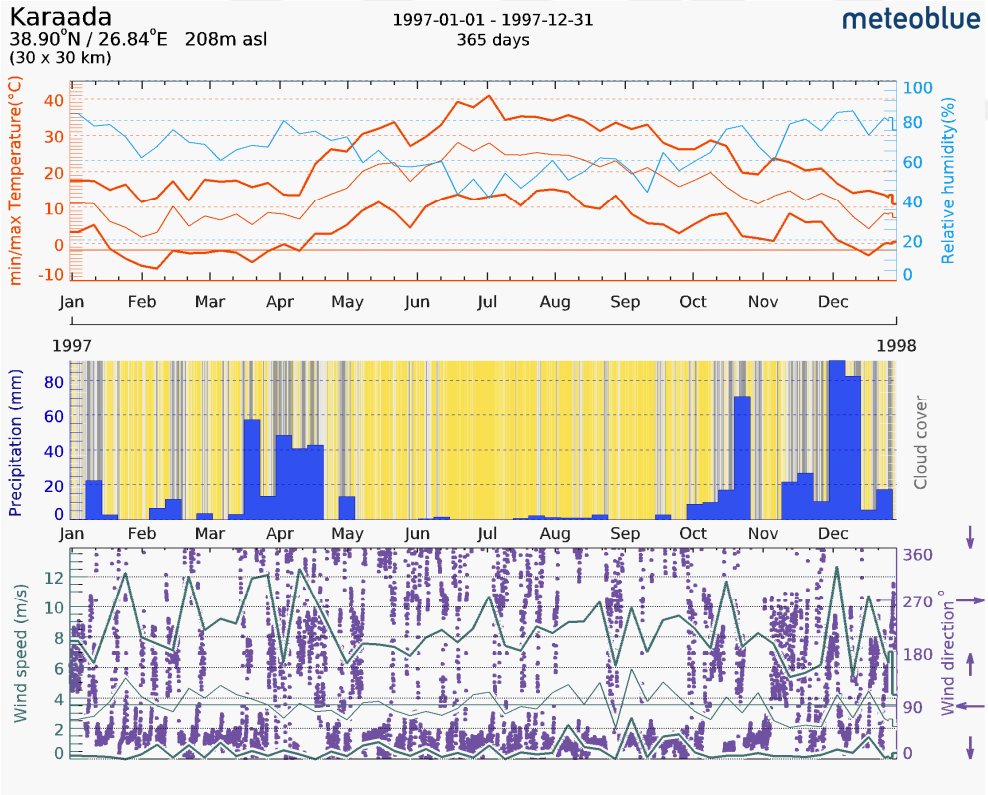
Karaada
38.90°N / 26.84°E 208m asl
(30 x 30 km)
1997-01-01 - 1997-12-31
365 days
meteoblue
min/max Temperature(°C)
Relative humidity(%)
Jan Feb Mar Apr May Jun Jul Aug Sep Oct Nov Dec
1997
1998
Precipitation (mm)
Cloud cover
Wind speed (m/s)
Wind direction °

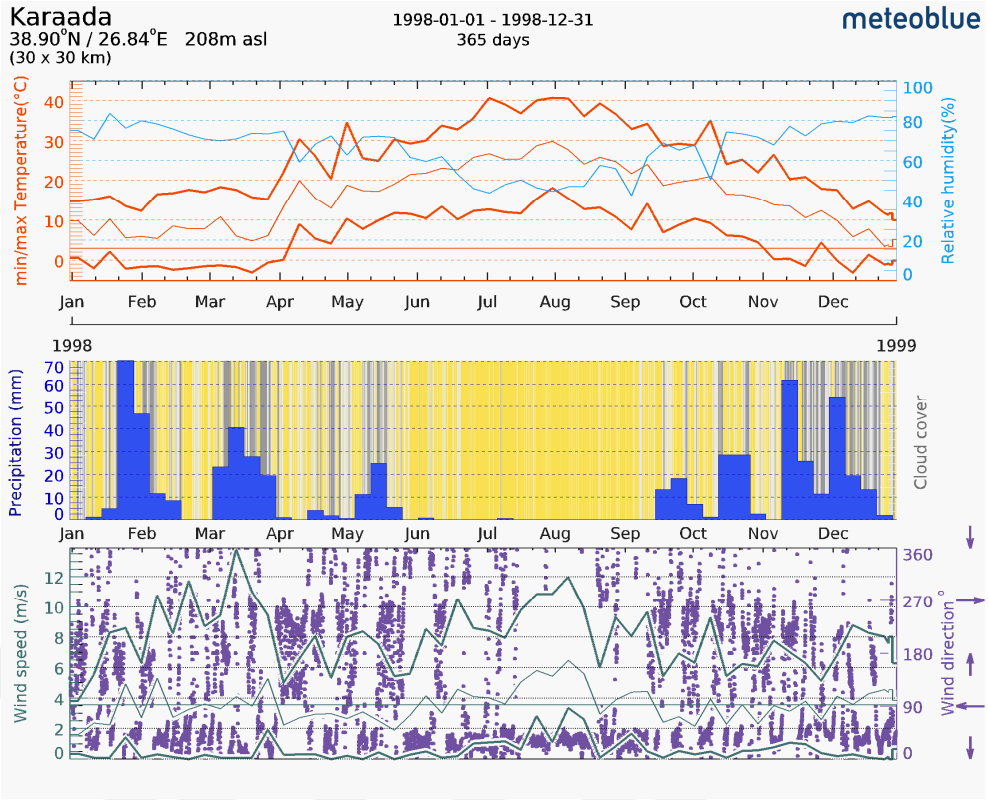
Karaada
38.90°N / 26.84°E 208m asl
(30 x 30 km)
1998-01-01 - 1998-12-31
365 days
meteoblue
min/max Temperature(°C)
Relative humidity(%)
Jan Feb Mar Apr May Jun Jul Aug Sep Oct Nov Dec
1998
1999
Precipitation (mm)
Cloud cover
Wind speed (m/s)
Wind direction °

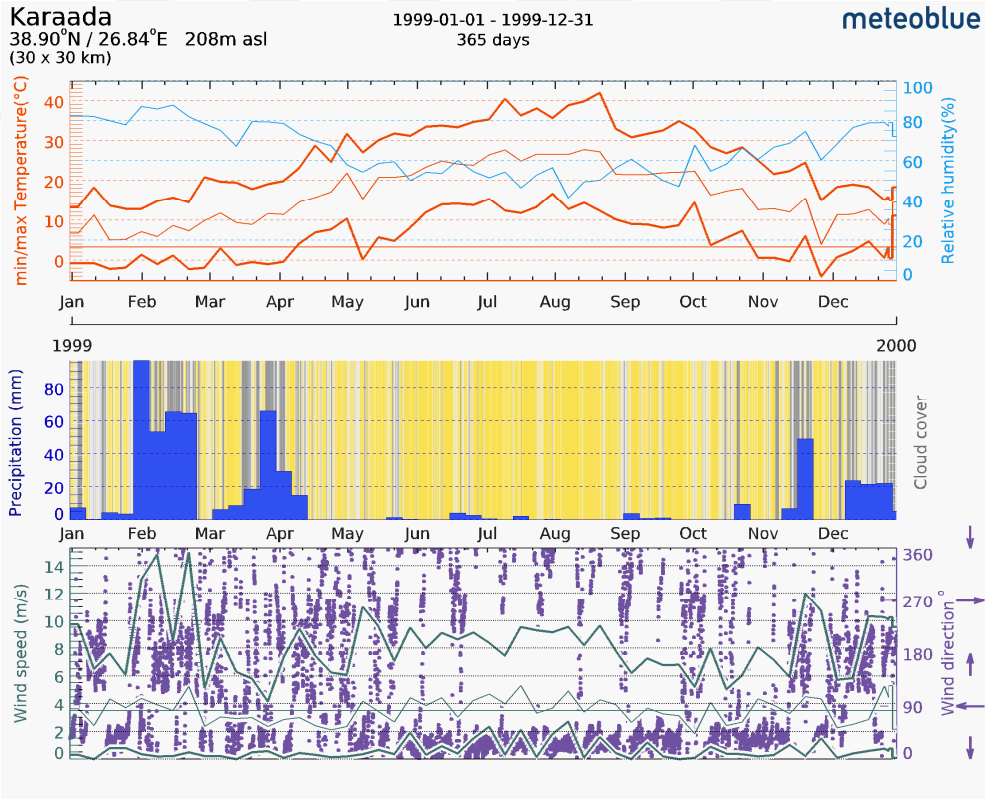
Karaada
38.90°N / 26.84°E 208m asl
(30 x 30 km)
1999-01-01 - 1999-12-31
365 days
meteoblue
min/max Temperature(°C)
Relative humidity(%)
Jan Feb Mar Apr May Jun Jul Aug Sep Oct Nov Dec
1999
2000
Precipitation (mm)
Cloud cover
Wind speed (m/s)
Wind direction °

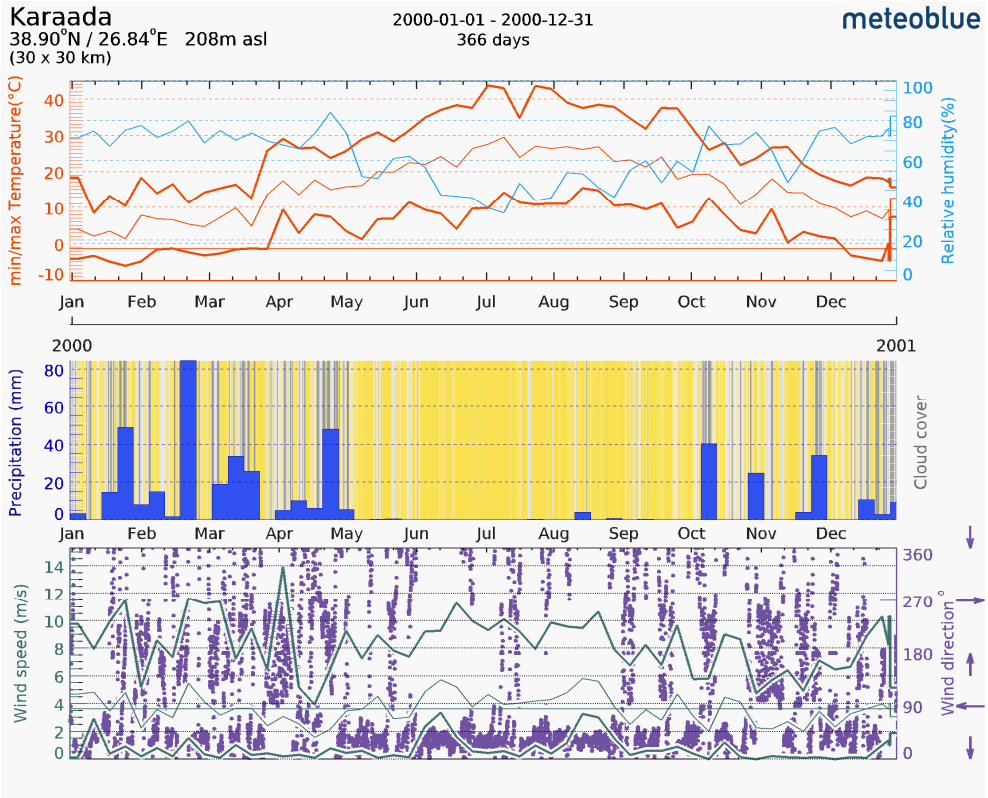
Karaada
38.90°N / 26.84°E 208m asl
(30 x 30 km)
2000-01-01 - 2000-12-31
366 days
meteoblue
min/max Temperature(°C)
Relative humidity(%)
Jan Feb Mar Apr May Jun Jul Aug Sep Oct Nov Dec
2000
2001
Precipitation (mm)
Cloud cover
Wind speed (m/s)
Wind direction °

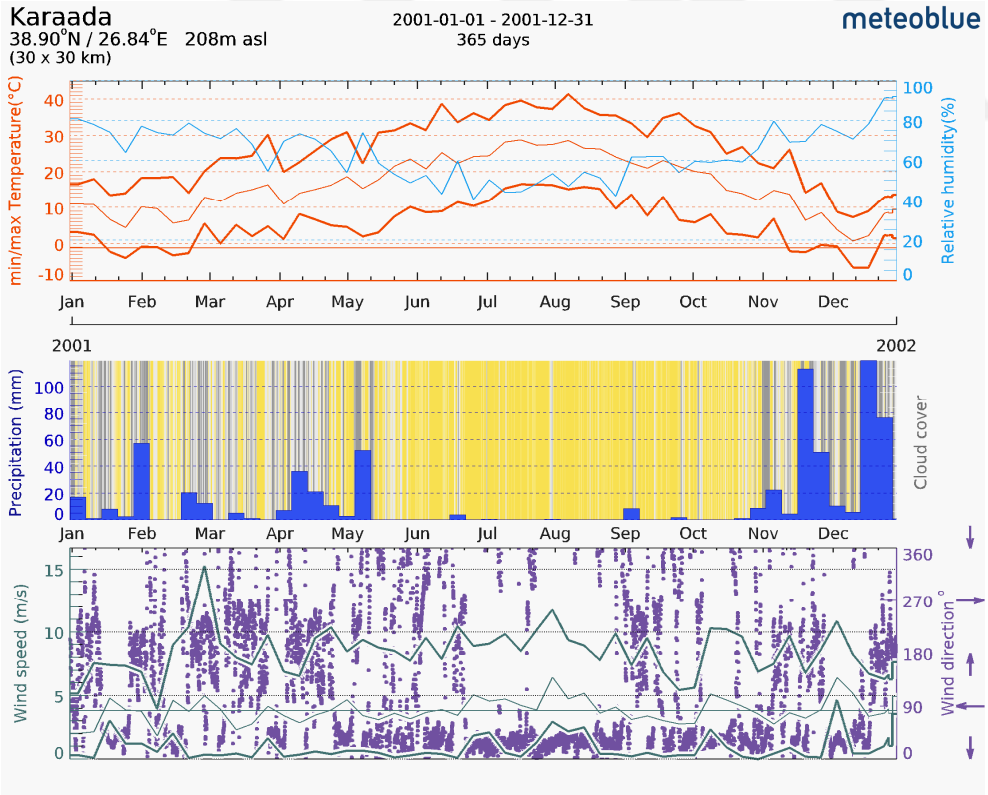
Karaada
38.90°N / 26.84°E 208m asl
(30 x 30 km)
2001-01-01 - 2001-12-31
365 days
meteoblue
min/max Temperature(°C)
Relative humidity(%)
Jan Feb Mar Apr May Jun Jul Aug Sep Oct Nov Dec
2001
2002
Precipitation (mm)
Cloud cover
Wind speed (m/s)
Wind direction °

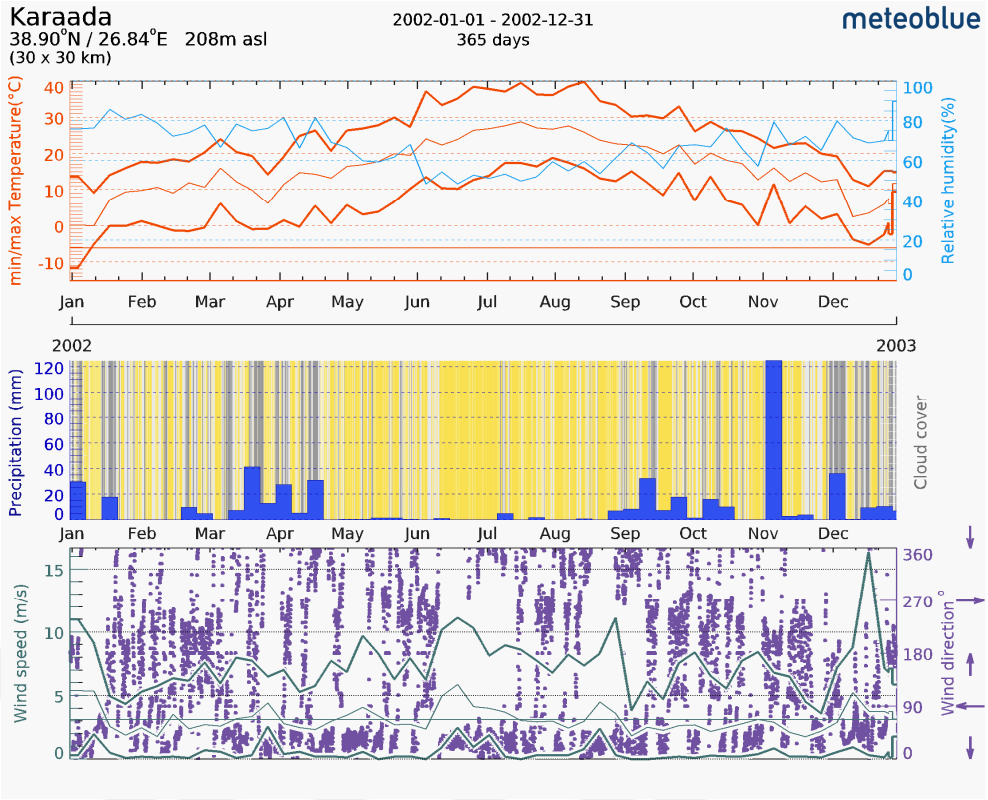
Karaada
38.90°N / 26.84°E 208m asl
(30 x 30 km)
2002-01-01 - 2002-12-31
365 days
meteoblue
min/max Temperature(°C)
Relative humidity(%)
Jan Feb Mar Apr May Jun Jul Aug Sep Oct Nov Dec
2002
2003
Precipitation (mm)
Cloud cover
Wind speed (m/s)
Wind direction °

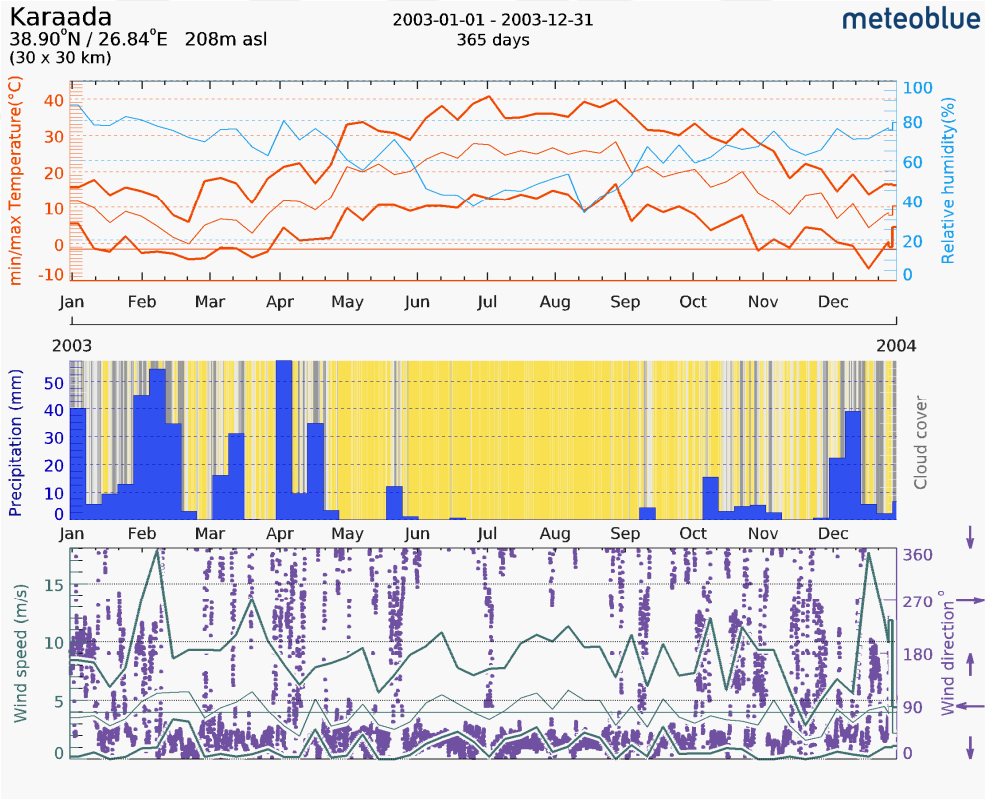
Karaada
38.90°N / 26.84°E 208m asl
(30 x 30 km)
2003-01-01 - 2003-12-31
365 days
meteoblue
min/max Temperature(°C)
Relative humidity(%)
Jan Feb Mar Apr May Jun Jul Aug Sep Oct Nov Dec
2003
2004
Precipitation (mm)
Cloud cover
Wind speed (m/s)
Wind direction °

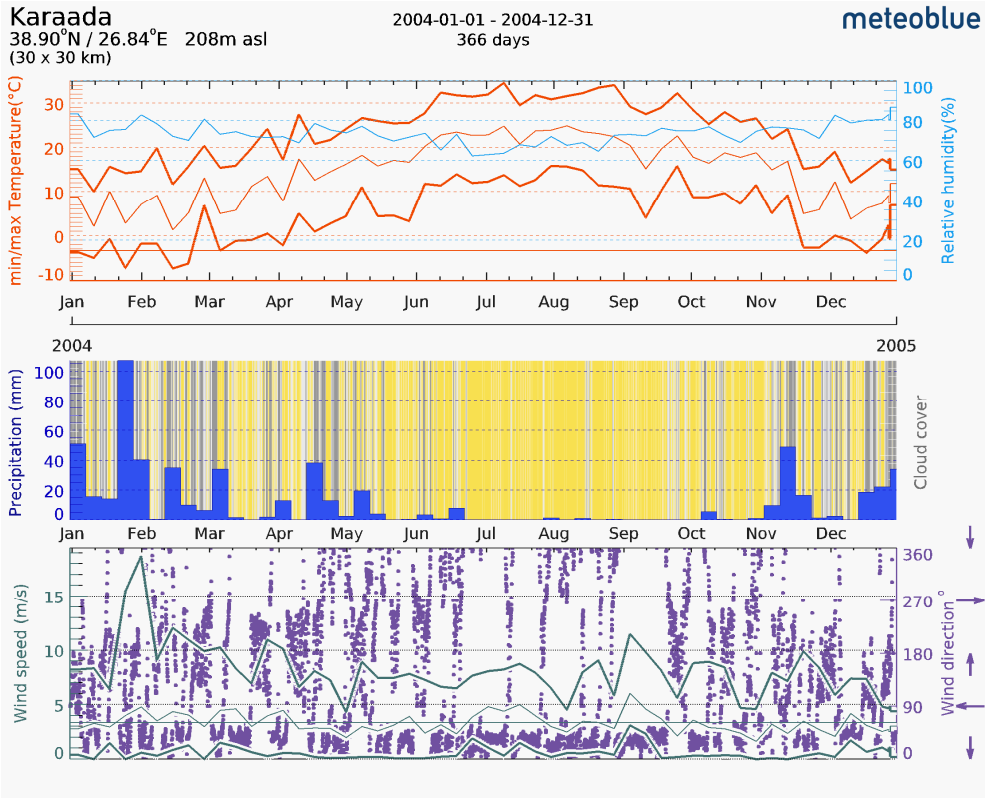
Karaada
38.90°N / 26.84°E 208m asl
(30 x 30 km)
2004-01-01 - 2004-12-31
366 days
meteoblue
min/max Temperature(°C)
Relative humidity(%)
Jan Feb Mar Apr May Jun Jul Aug Sep Oct Nov Dec
2004
2005
Precipitation (mm)
Cloud cover
Wind speed (m/s)
Wind direction °

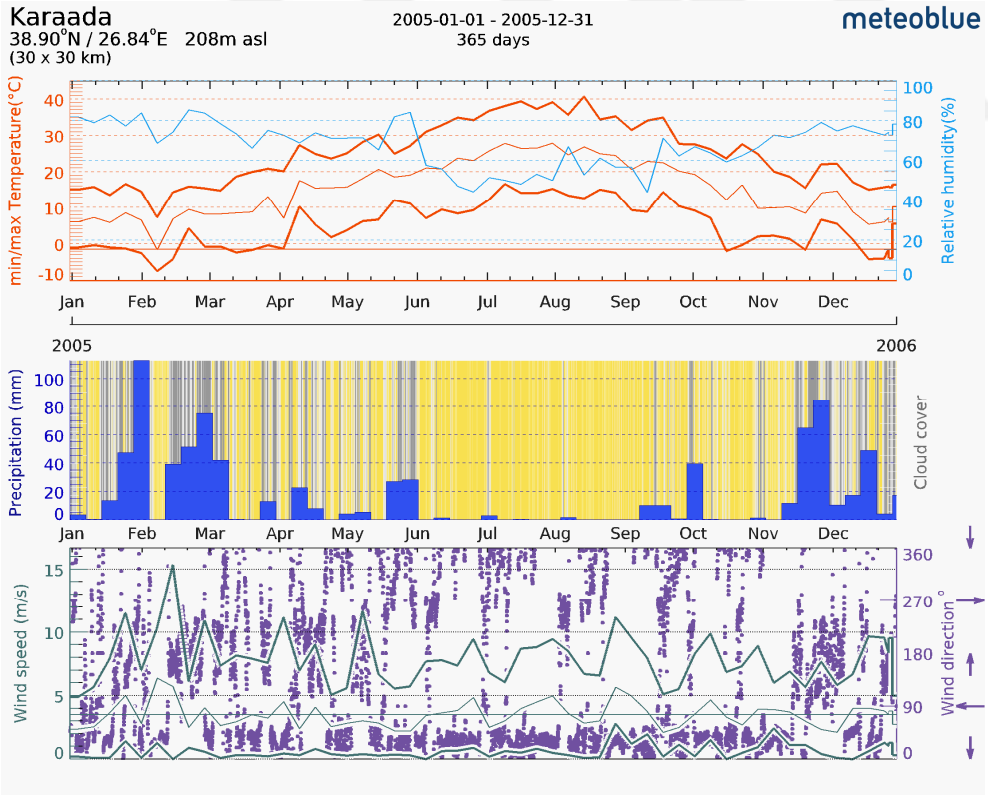
Karaada
38.90°N / 26.84°E 208m asl
(30 x 30 km)
2005-01-01 - 2005-12-31
365 days
meteoblue
min/max Temperature(°C)
Relative humidity(%)
Jan Feb Mar Apr May Jun Jul Aug Sep Oct Nov Dec
2005
2006
Precipitation (mm)
Cloud cover
Wind speed (m/s)
Wind direction °

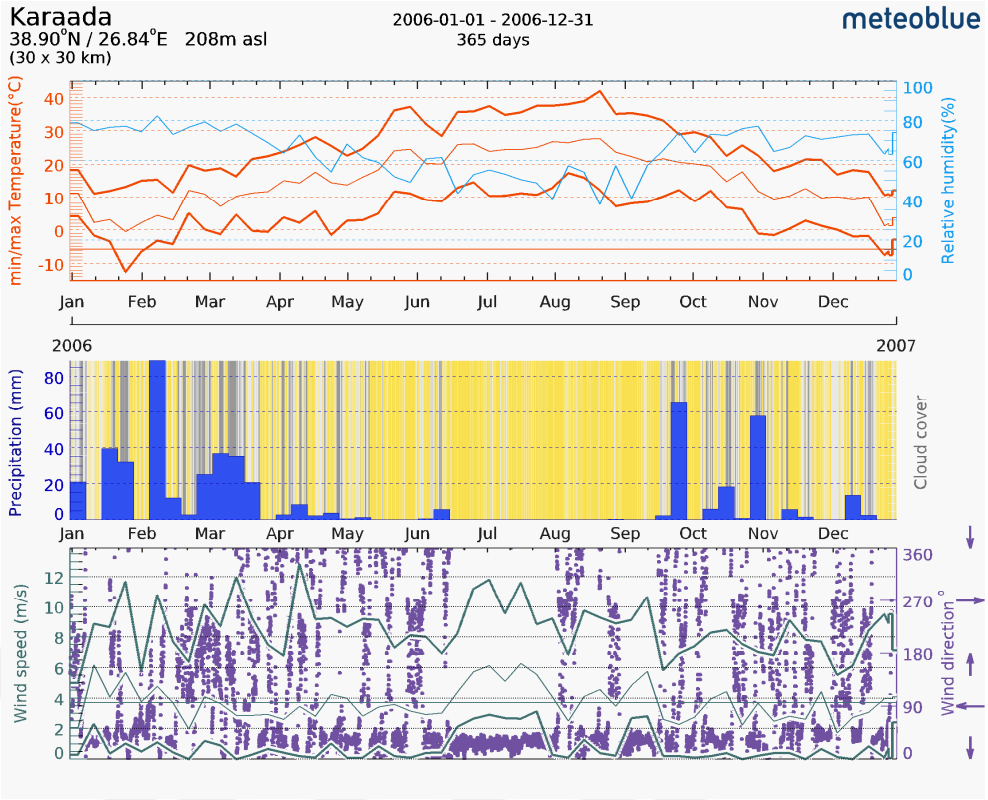
Karaada
38.90°N / 26.84°E 208m asl
(30 x 30 km)
2006-01-01 - 2006-12-31
365 days
meteoblue
min/max Temperature(°C)
Relative humidity(%)
Jan Feb Mar Apr May Jun Jul Aug Sep Oct Nov Dec
2006
2007
Precipitation (mm)
Cloud cover
Wind speed (m/s)
Wind direction °

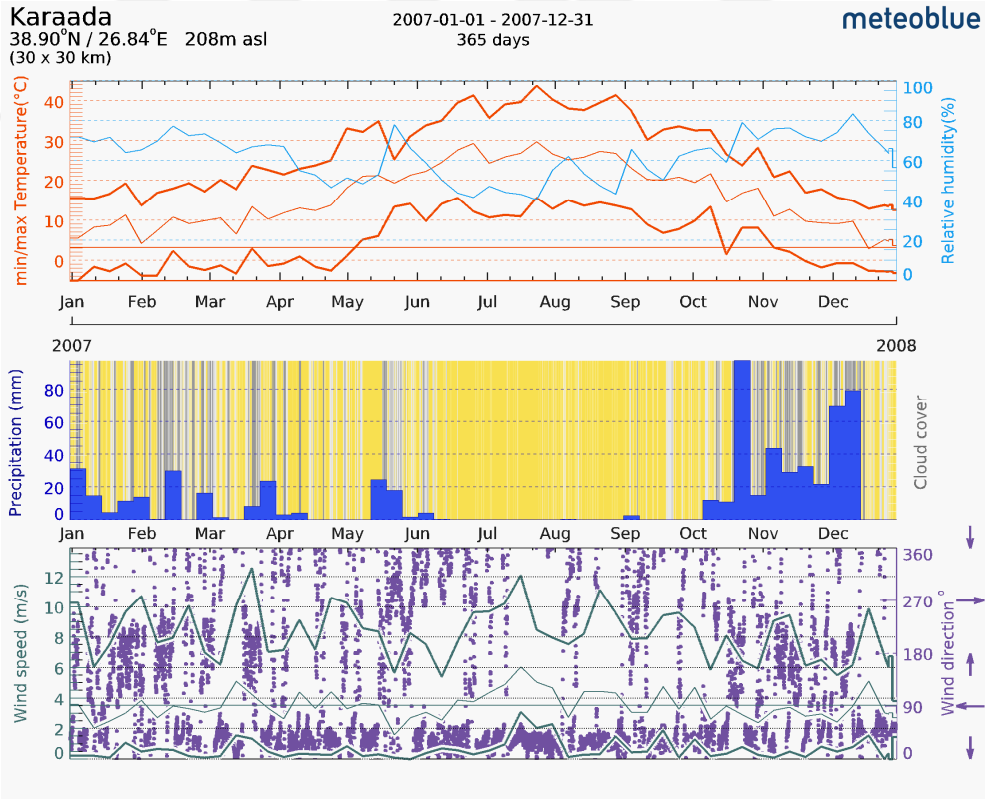
Karaada
38.90°N / 26.84°E 208m asl
(30 x 30 km)
2007-01-01 - 2007-12-31
365 days
meteoblue
min/max Temperature(°C)
Relative humidity(%)
Jan Feb Mar Apr May Jun Jul Aug Sep Oct Nov Dec
2007
2008
Precipitation (mm)
Cloud cover
Wind speed (m/s)
Wind direction °

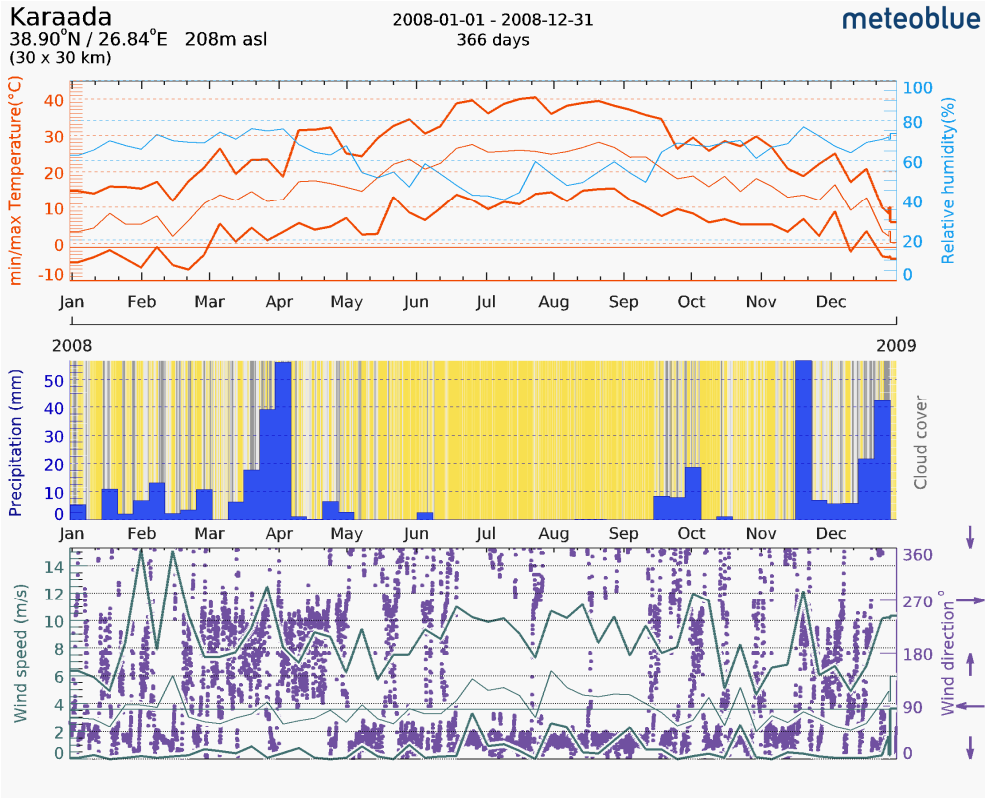
Karaada
38.90°N / 26.84°E 208m asl
(30 x 30 km)
2008-01-01 - 2008-12-31
366 days
meteoblue
min/max Temperature(°C)
Relative humidity(%)
Jan Feb Mar Apr May Jun Jul Aug Sep Oct Nov Dec
2008
2009
Precipitation (mm)
Cloud cover
Wind speed (m/s)
Wind direction °

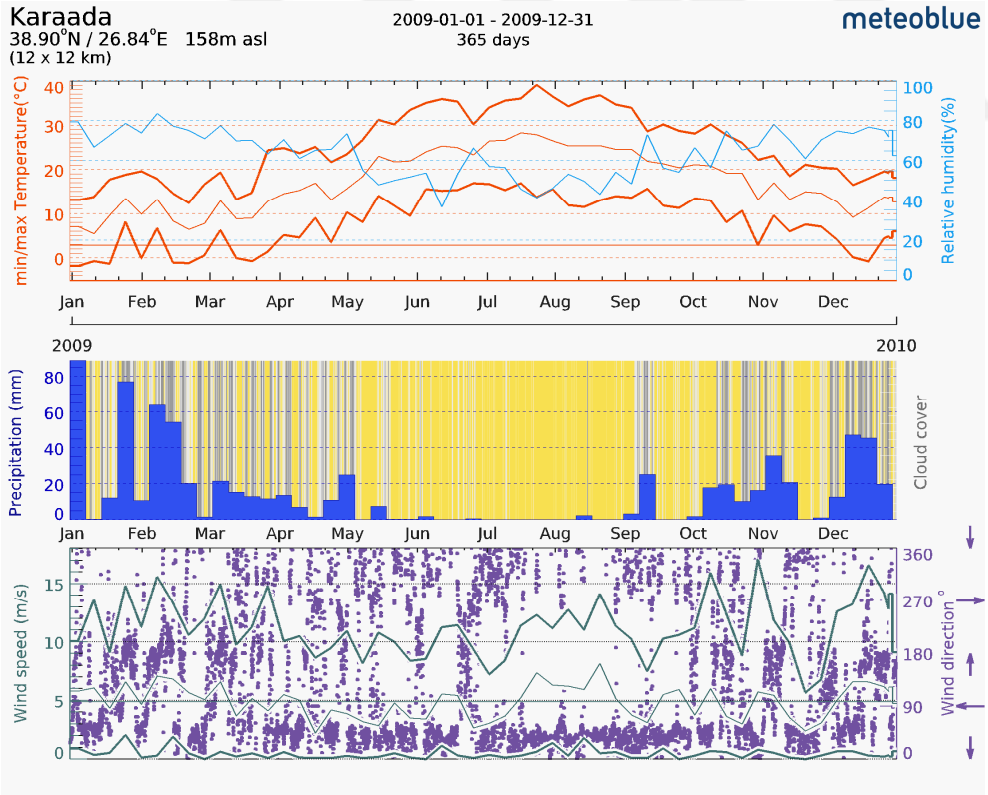
Karaada
38.90°N / 26.84°E 158m asl
(12 x 12 km)
2009-01-01 - 2009-12-31
365 days
meteoblue
min/max Temperature(°C)
Relative humidity(%)
Jan Feb Mar Apr May Jun Jul Aug Sep Oct Nov Dec
2009
2010
Precipitation (mm)
Cloud cover
Wind speed (m/s)
Wind direction °

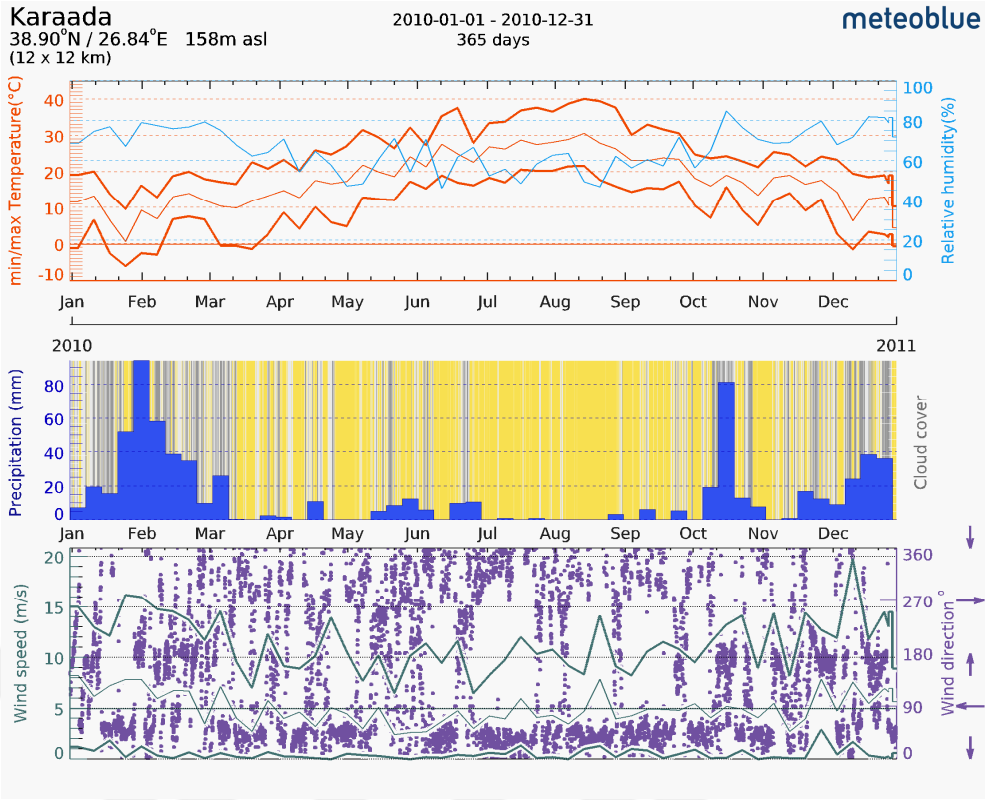
Karaada
38.90°N / 26.84°E 158m asl
(12 x 12 km)
2010-01-01 - 2010-12-31
365 days
meteoblue
min/max Temperature(°C)
Relative humidity(%)
Jan Feb Mar Apr May Jun Jul Aug Sep Oct Nov Dec
2010
2011
Precipitation (mm)
Cloud cover
Wind speed (m/s)
Wind direction °

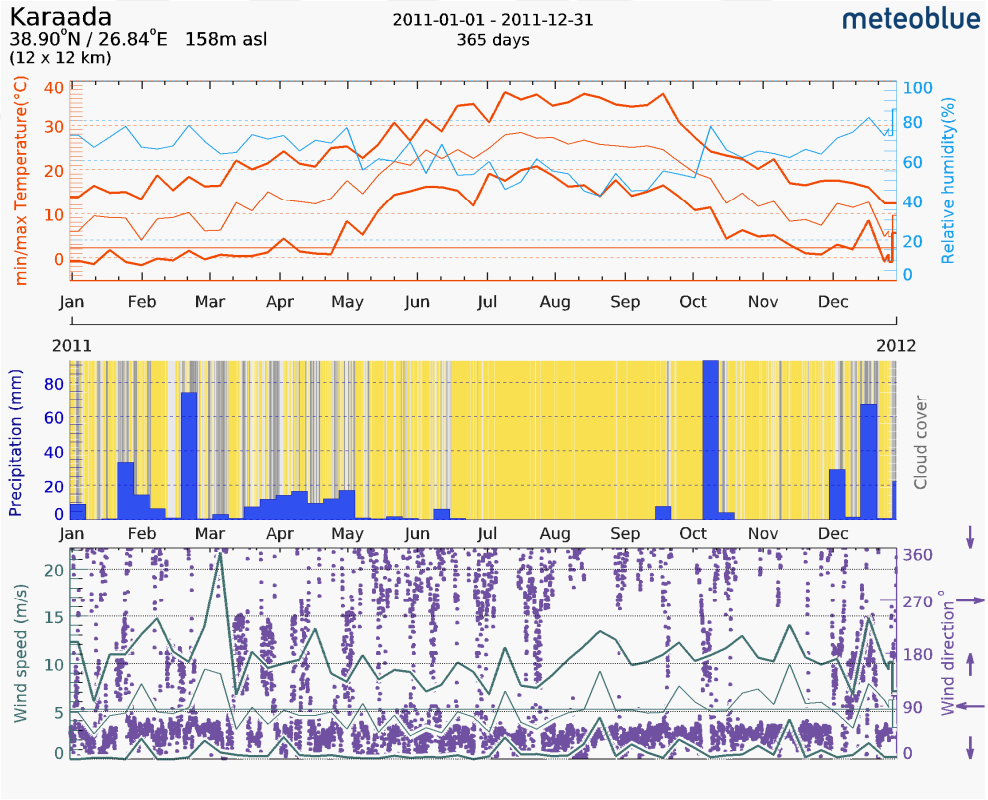
Karaada
38.90°N / 26.84°E 158m asl
(12 x 12 km)
2011-01-01 - 2011-12-31
365 days
meteoblue
min/max Temperature(°C)
Relative humidity(%)
Jan Feb Mar Apr May Jun Jul Aug Sep Oct Nov Dec
2011
2012
Precipitation (mm)
Cloud cover
Wind speed (m/s)
Wind direction °

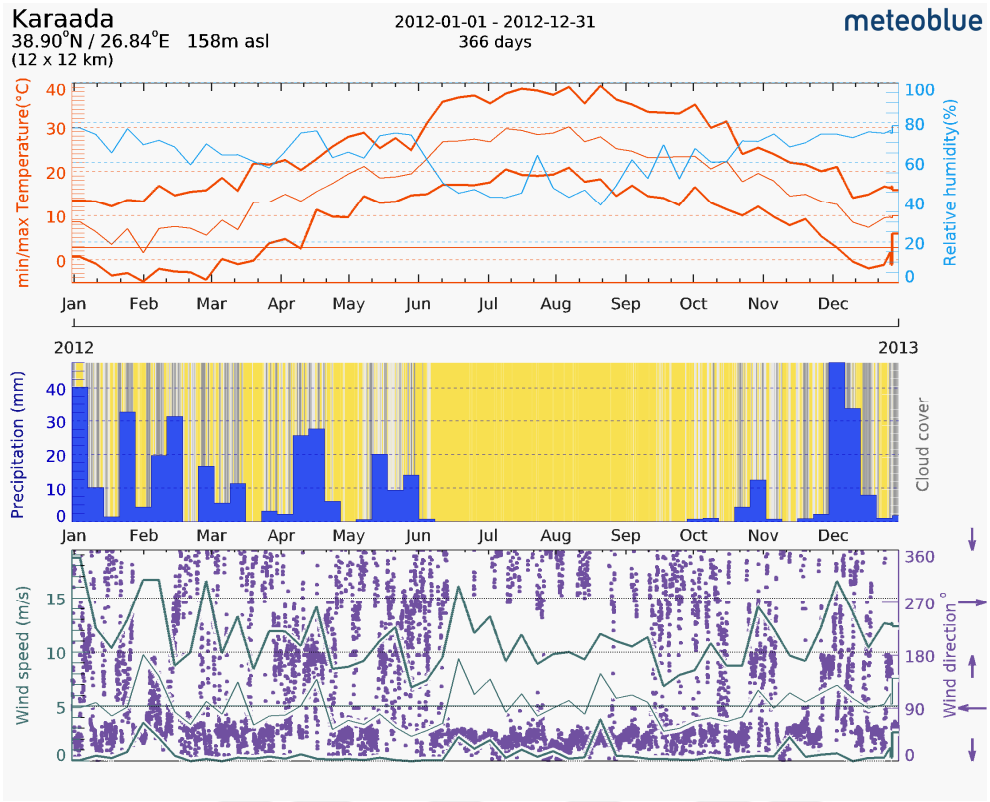
Karaada
38.90°N / 26.84°E 158m asl
(12 x 12 km)
2012-01-01 - 2012-12-31
366 days
meteoblue
min/max Temperature(°C)
Relative humidity(%)
Jan Feb Mar Apr May Jun Jul Aug Sep Oct Nov Dec
2012
2013
Precipitation (mm)
Cloud cover
Wind speed (m/s)
Wind direction °

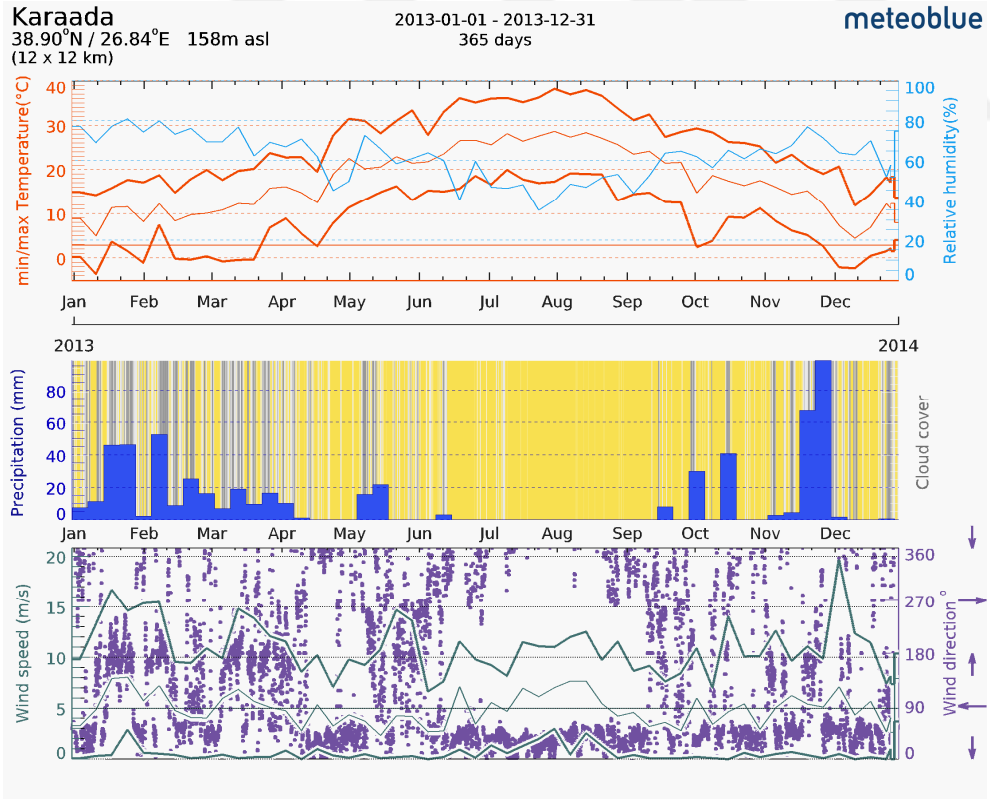
Karaada
38.90°N / 26.84°E 158m asl
(12 x 12 km)
2013-01-01 - 2013-12-31
365 days
meteoblue
min/max Temperature(°C)
Relative humidity(%)
Jan Feb Mar Apr May Jun Jul Aug Sep Oct Nov Dec
2013
2014
Precipitation (mm)
Cloud cover
Wind speed (m/s)
Wind direction °

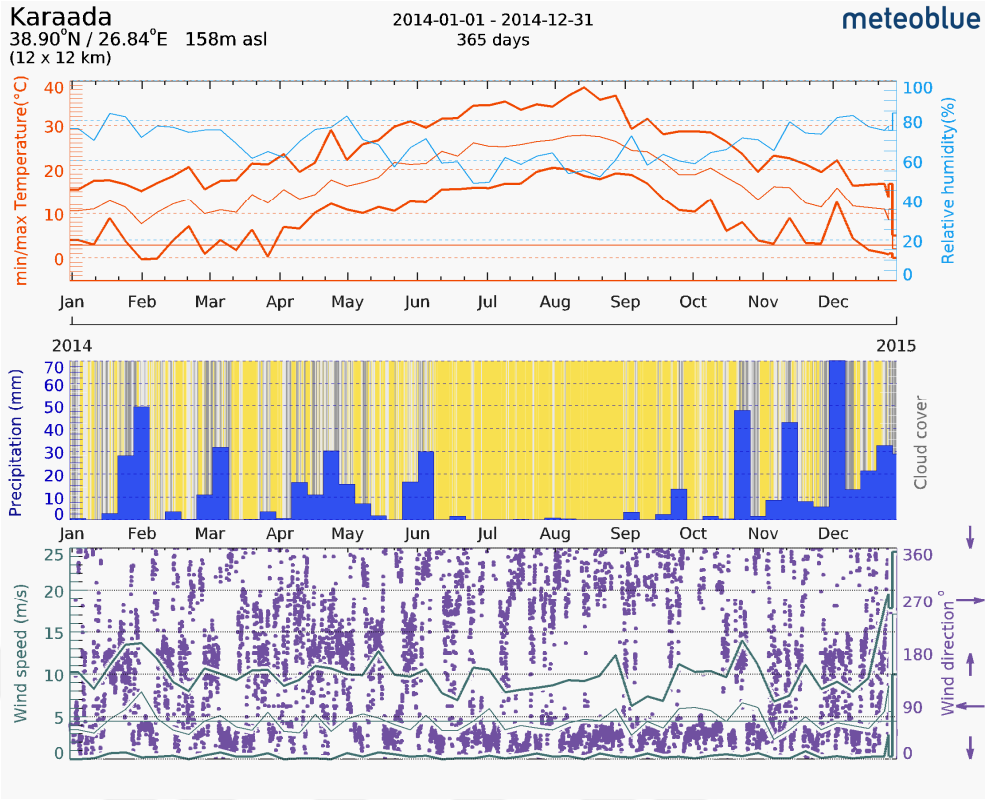
Karaada
38.90°N / 26.84°E 158m asl
(12 x 12 km)
2014-01-01 - 2014-12-31
365 days
meteoblue
min/max Temperature(°C)
Relative humidity(%)
Jan Feb Mar Apr May Jun Jul Aug Sep Oct Nov Dec
2014
2015
Precipitation (mm)
Cloud cover
Wind speed (m/s)
Wind direction °

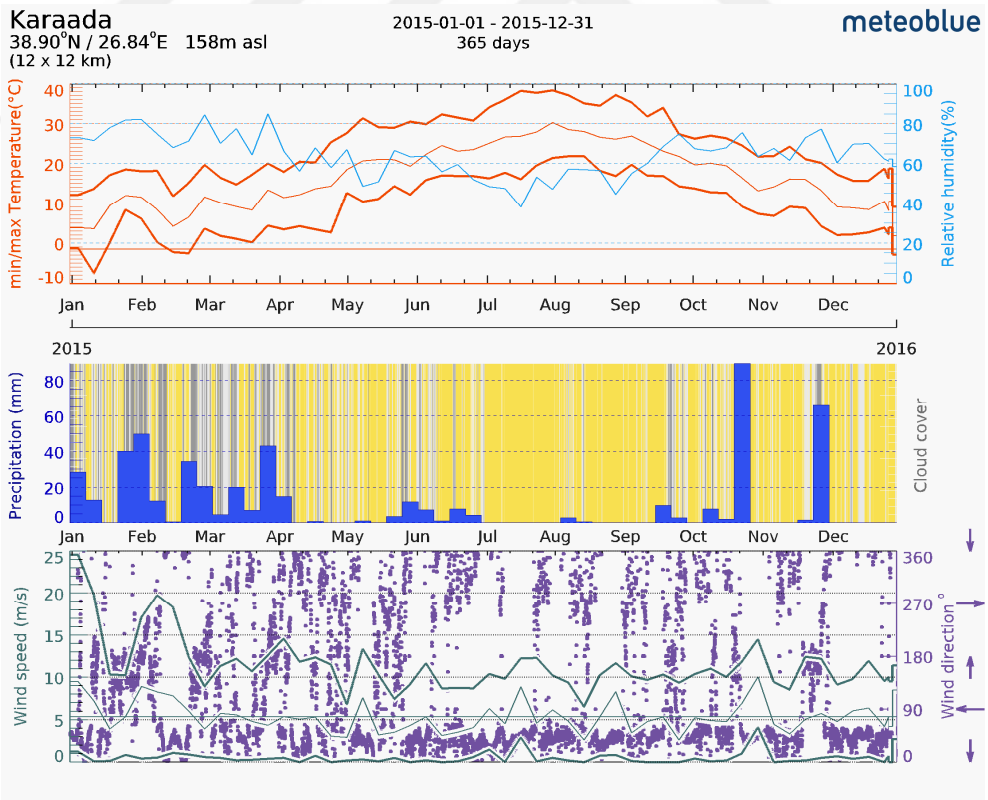
Karaada
38.90°N / 26.84°E 158m asl
(12 x 12 km)
2015-01-01 - 2015-12-31
365 days
meteoblue
min/max Temperature(°C)
Relative humidity(%)
Jan Feb Mar Apr May Jun Jul Aug Sep Oct Nov Dec
2015
2016
Precipitation (mm)
Cloud cover
Wind speed (m/s)
Wind direction °

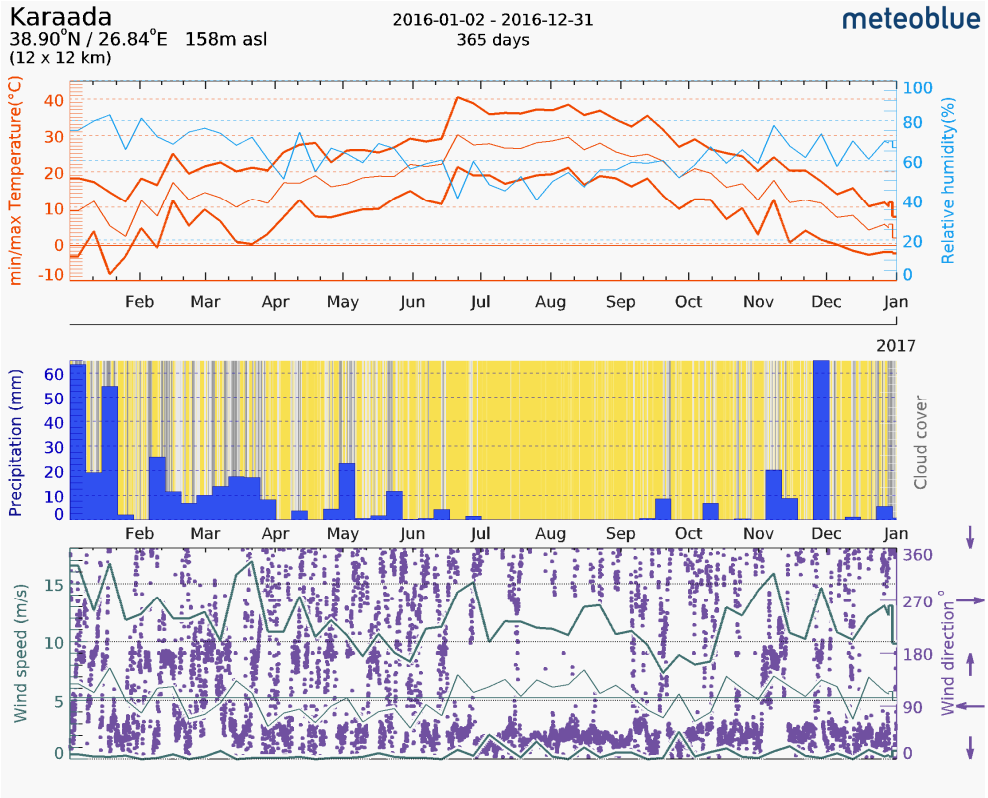
Karaada
38.90°N / 26.84°E 158m asl
(12 x 12 km)
2016-01-02 - 2016-12-31
365 days
meteoblue
min/max Temperature(°C)
Relative humidity(%)
Feb Mar Apr May Jun Jul Aug Sep Oct Nov Dec Jan
2017
Precipitation (mm)
Cloud cover
Wind speed (m/s)
Wind direction °

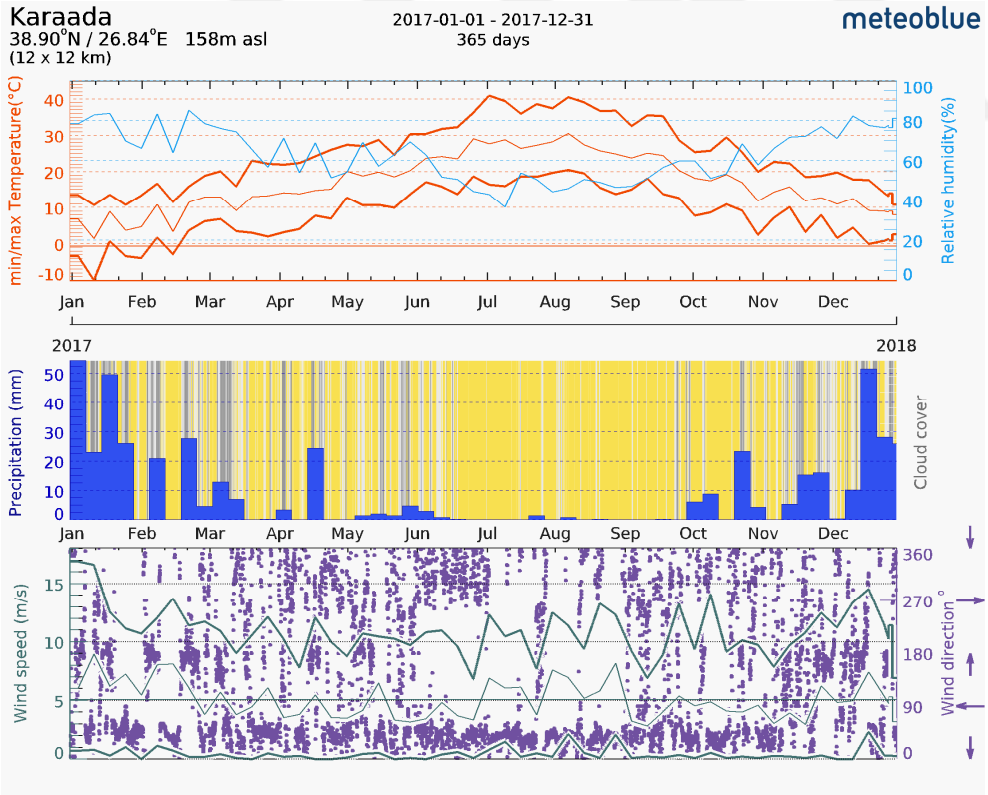
Karaada
38.90°N / 26.84°E 158m asl
(12 x 12 km)
2017-01-01 - 2017-12-31
365 days
meteoblue
min/max Temperature(°C)
Relative humidity(%)
Jan Feb Mar Apr May Jun Jul Aug Sep Oct Nov Dec
2017
2018
Precipitation (mm)
Cloud cover
Wind speed (m/s)
Wind direction °

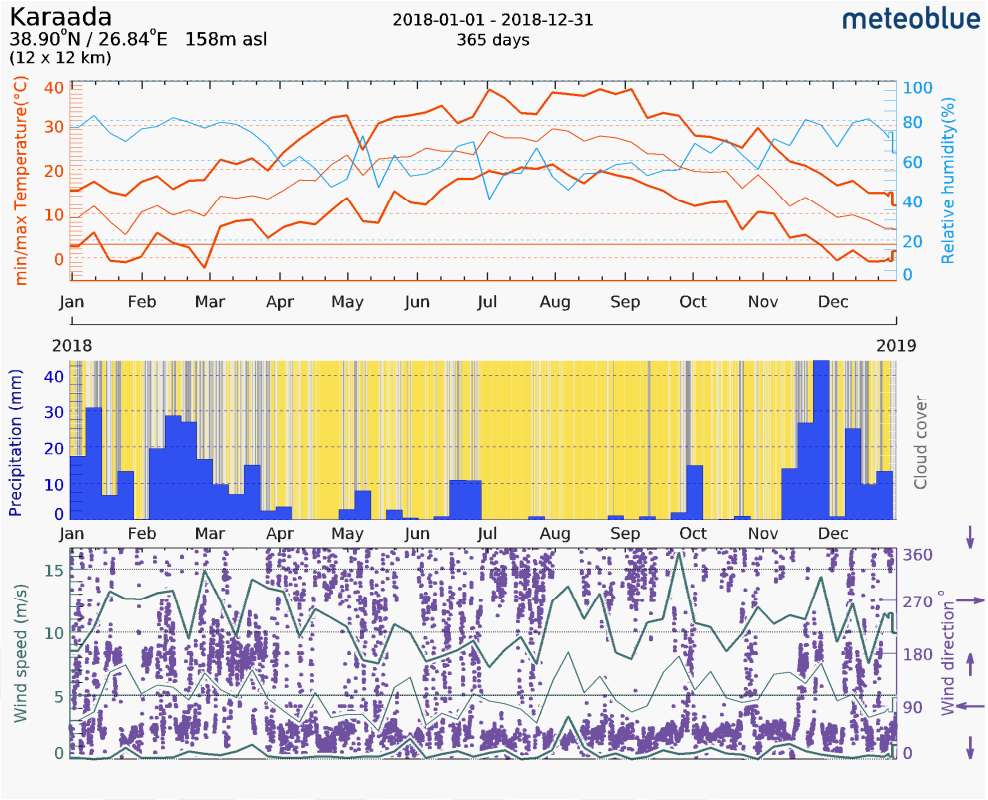
Karaada
38.90°N / 26.84°E 158m asl
(12 x 12 km)
2018-01-01 - 2018-12-31
365 days
meteoblue
min/max Temperature(°C)
Relative humidity(%)
Jan Feb Mar Apr May Jun Jul Aug Sep Oct Nov Dec
2018
2019
Precipitation (mm)
Cloud cover
Wind speed (m/s)
Wind direction °

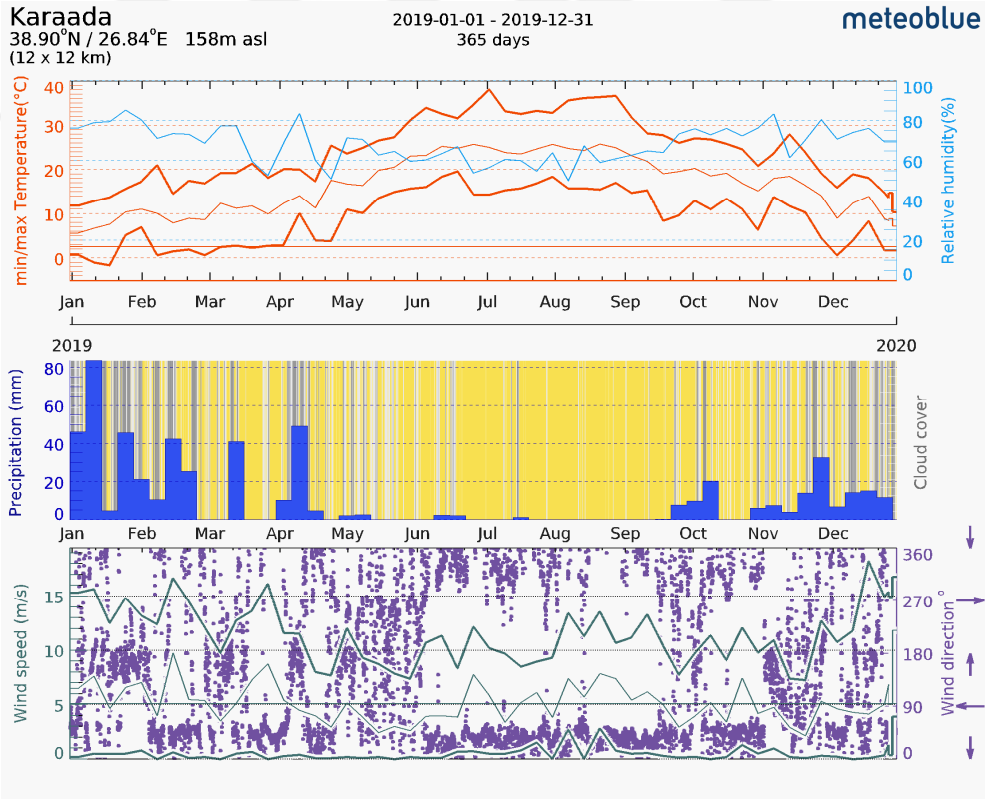
Karaada
38.90°N / 26.84°E 158m asl
(12 x 12 km)
2019-01-01 - 2019-12-31
365 days
meteoblue
min/max Temperature(°C)
Relative humidity(%)
Jan Feb Mar Apr May Jun Jul Aug Sep Oct Nov Dec
2019
2020
Precipitation (mm)
Cloud cover
Wind speed (m/s)
Wind direction °

APPENDIX B

The Meteoblue weather archive diagrams show simulation data for the selected location. The diagrams show hourly data. There are daily aggregations for minimum, maximum and average values over a month. The weather archive diagrams are divided into three charts:

1) Minimum, maximum and average temperature (orange lines), including relative humidity (blue line).
2) Precipitation amount (blue bars), clouds (gray background) and clear sky (yellow background).
3) Minimum, maximum and average wind speed (green lines) and wind direction (purple points) are specified in degrees: 0° = North, 90° = East, 180° = South, 270° = West.

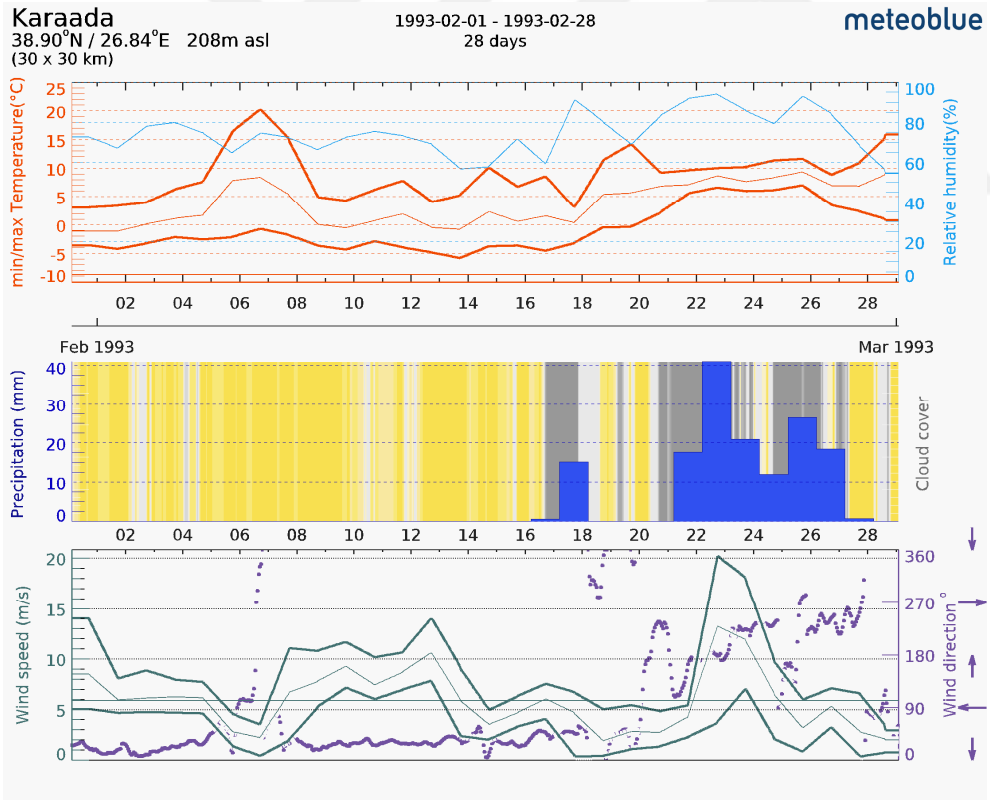

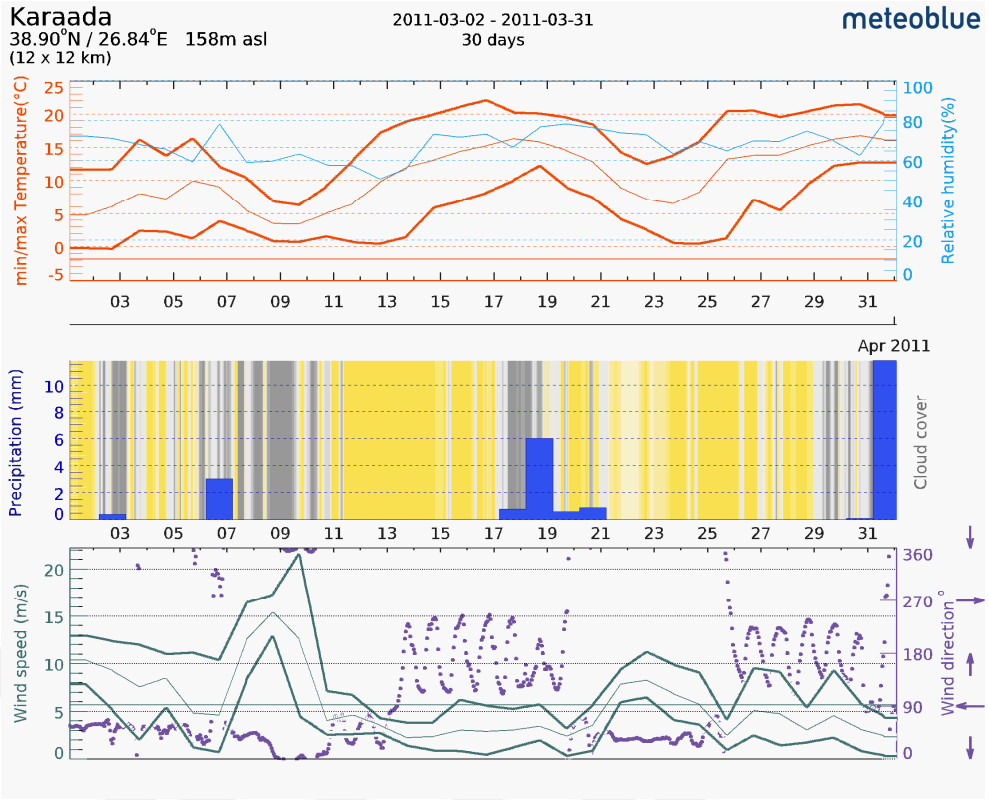
Karaada
38.90°N / 26.84°E 158m asl
(12 x 12 km)
2011-03-02 - 2011-03-31
30 days
meteoblue
min/max Temperature(°C)
Relative humidity(%)
Apr 2011
Precipitation (mm)
Cloud cover
Wind speed (m/s)
Wind direction°

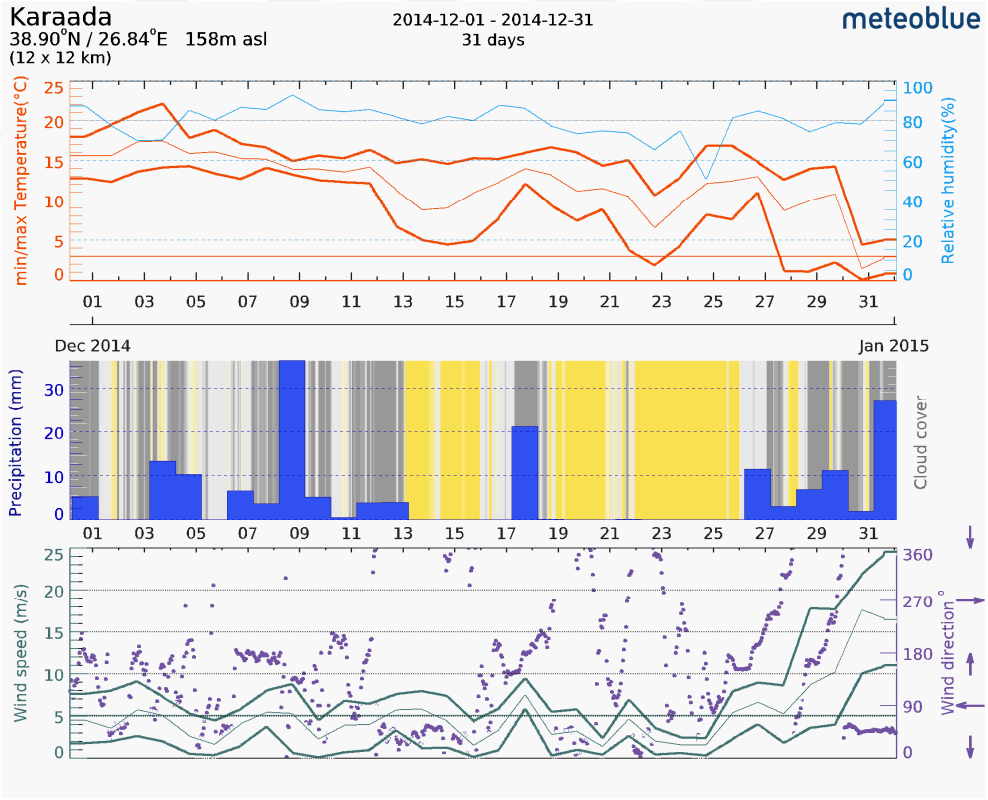
Karaada
38.90°N / 26.84°E 158m asl
(12 x 12 km)
2014-12-01 - 2014-12-31
31 days
meteoblue
min/max Temperature(°C)
Relative humidity(%)
Dec 2014
Jan 2015
Precipitation (mm)
Cloud cover
Wind speed (m/s)
Wind direction°

CURRICULUM VITAE

Name Surname **:** Erdem ACAR

EDUCATION

- **B.Sc.** **:** 2002, ITU, Faculty of Naval Architecture and Ocean Engineering, Department of Ocean Engineering.
- **M.Sc.** **:** 2014, ITU, Energy Institute, Energy Science and Technology Programme.